Temporal Analysis of Forest Cover Change and Landslides Susceptibility Mapping along Karakoram Highway Using Geographic Information System and Remote Sensing

Barira Rashid

(2015-NUST-MS-GIS-119774)

A thesis submitted in partial fulfillment of the requirements for the degree of Master of Science in Remote Sensing and GIS

Institute of Geographical Information Systems
School of Civil and Environmental Engineering
National University of Sciences & Technology
Islamabad, Pakistan

August, 2018

Temporal Analysis of Forest Cover Change and Landslides Susceptibility Mapping along Karakoram Highway Using Geographic Information System and Remote Sensing

Author

BARIRA RASHID

Regn Number

119774

A thesis submitted in partial fulfillment of the requirements for the degree

of

MS GIS and Remote Sensing

Thesis Supervisor:

Dr. Javed Iqbal

Thesis Supervisor's Signature: ___________________________________

INSTITUTE OF GEOGRAPHIC INFORMATION SYSTEM

SCHOOL OF CIVIL AND ENVIRONMENTAL

ENGINEERING

NATIONAL UNIVERSITY OF SCIENCES AND

TECHNOLOGY,

ISLAMABAD

August 27, 2018

THESIS ACCEPTANCE CERTIFICATE

Certified that final copy of MS/MPhil thesis written by Miss Barira Rashid _ (Registration No. 119774), of Institute of Geographic Information System, SCEE has been vetted by undersigned, found complete in all respects as per NUST statutes/Regulations, is free of plagiarism, errors and mistakes and is accepted as partial fulfillment for award of MS/MPhil degree. It is further certified that necessary amendments as pointed out by GEC members of the scholar have also been incorporated in the said thesis.

Signature: ______________________________

Name of Supervisor: _____Dr. Javed Iqbal___________

Date: ______________________________

Signature (HOD): ______________________________

Date: ______________________________

Signature(Dean/Principal): ______________________________

Date: ______________________________

CERTIFICATE

It is certified that the content and form of this thesis entitled **"Temporal Analysis of Forest Cover Change and Landslides Susceptibility Mapping along Karakoram Highway Using Geographic Information System and Remote Sensing"** submitted by **"Barira Rashid"** have been found satisfactory for the requirement of the Master of Science degree in Remote Sensing and Geographical Information Systems.

Supervisor: ____________________

Name: Dr. Javed Iqbal

Designation: (Associate Professor. / Head of Department., IGIS)

Members of Guidance and Examination Committee

Member: ____________________

Name: Mr. Junaid Aziz Khan

Designation: Lecturer., IGIS

Member: ____________________

Name: **Dr. Ejaz Hussain**

Designation: Associate Dean, IGIS

External Examiner: __________________

Name: Dr. Abdul Waheed

Designation: Assistant Professor, NIT

ACADEMIC THESIS: DECLARATION OF AUTHORSHIP

I, **Barira Rashid**, declare that this thesis and the work presented in it are my own and have been generated by me as the result of my own original research.

Temporal Analysis of Forest Cover Change and Landslides Susceptibility Mapping along Karakoram Highway Using Geographic Information System and Remote Sensing

I confirm that:

1. This thesis is composed of my original work, and contains no material previously published or written by another person except where due reference has been made in the text;
2. Wherever any part of this thesis has previously been submitted for a degree or any other qualification at this or any other institution, it has been clearly stated;
3. I have acknowledged all main sources of help;
4. Where the thesis is based on work done by myself jointly with others, I have made clear exactly what was done by others and what I have contributed myself;
5. None of this work has been published before submission.
6. This work is not plagiarized under the HEC plagiarism policy.

Signed: ……………………………

Date: ……27/08/2018………………

Plagiarism Certificate (Turnitin Report)

This thesis has been checked for Plagiarism. Turnitin report endorsed by Supervisor is attached.

Signature of Student

Barira Rashid

119774

Signature of Supervisor

Acknowledgments

First and foremost, I'd like to bow my head in gratitude to the Allah Almighty, for enabling me to have completed this research with His blessings.

I'd like to express my deep and sincerest gratitude to my thesis advisor, Dr. Javed Iqbal, Associate Professor and Head of Department, IGIS, NUST, for providing invaluable guidance, advice, creativity, constructive criticism and keen interest in my research work. I'm thankful to him for giving me the opportunity to learn from his experience and having confidence in me. I am indebted to National University of Sciences and Technology (NUST) for providing us a platform to have such an experience. Besides my supervisor, I would like to thank the rest of my thesis Guidance and Examination Committee: Mr. Junaid Aziz Khan, Dr. Ejaz Hussain and Dr. Abdul Waheed, for their insightful comments, and encouragement regarding the research. I am sincerely grateful to Mr. Junaid Aziz Khan for his timely advice and tireless efforts throughout the research phase.

I am extremely grateful to my parents for their prayers, love and sacrifices for educating me and preparing for my future. Many thanks to my siblings and colleagues for their prayers, support and patience throughout my research. I would like to thank Jawairia Waqas and Sahaab Farooq for their expert advice and guidance in my work. I'd like to thank Daud Kamal for pictures courtesy for this research. I feel great pleasure in expressing my gratitude to my friends Asma Rashid, Ali Taha, and Ghulam Ayesha for their unconditional support and for being there whenever I needed. A heap of thanks to all my friends and batch mates for the time we spent together and shared the knowledge, joy and hard time.

The research is a complete mixed package that is directly or indirectly involving the contribution of many personalities. Therefore, I would like to express my gratitude to all the individuals who have rendered valuable assistance to my study.

Dedicated to my exceptional parents and adored siblings whose tremendous support and cooperation led me to this wonderful accomplishment

Table of Contents

LIST OF FIGURES .... **iii**

LIST OF TABLES .... **iv**

LIST OF ABBREVIATIONS .... **v**

ABSTRACT .... **vi**

Chapter 1 .... **1**

INTRODUCTION **1**

1.1.Background Information 1

1.2.Rationale 5

1.3.Objectives 6

1.4.The scope of the study 6

Chapter 2 .... **8**

MATERIALS AND METHODS **8**

2.1. Study Area 8

Physiography 9

Climate 9

Geology and Soil Composition 10

2.2. Dataset Used 10

Satellite Images 12

Digital Elevation Model(DEM) 12

Geological Map 12

Precipitation Map 13

2.3. Software Used 13

2.4. Methodology 13

2.4.1. Forest Cover Change Mapping 13

2.4.2. Landslide Susceptibility Methodology 16

Analytical Hierarchy Process 17

Weighted Linear Combination 20

Scoops 3D 20

Chapter 3 .... **23**

RESULTS AND DISCUSSIONS **23**

3.1. Forest Cover Change 23

3.2. Landslide Susceptibility Mapping Using AHP and WLC 25
Analytical Hierarchy Process and Weighted Linear Combination 30
Landslides Susceptibility using Scoops 3D 33
Interpretation of the Results with the association to KKH 42
***Chapter 4* 49**
CONCLUSION AND RECOMMENDATIONS 49
4.1. Conclusions 49
4.2. Recommendations for further research 51
REFERENCES 52
APPENDICES 58
Appendix I 58
Appendix II 60
Appendix II 63

LIST OF FIGURES

Figure 1. Study area map of Karakoram Highway (N-35) from Hasanabdal to Sazin. 11
Figure 2. Complete work flow chart for the identification of forest cover dynamics and landslide mapping. 15
Figure 3. Flowchart for mapping the forest cover dynamics from 1990 to 2016. 18
Figure 4. Landslide susceptibility mapping through AHP and Scoops model. 18
Figure 5. Forest cover dynamics along KKH from 1990 to 2016. 26
Figure 6. Spatiotemporal change of each LULC class from 1990 to 2016. 26
Figure 7. Causative Layers for AHP 31
a) Slope degrees, b) Lithology and the proximity, c) Precipitation, d) LULC, e) Plan Curvature and f) Aspect. 31
Figure 8. Landslide susceptibility map depicting susceptible zones. 39
Figure 9. Piechart of the landslide susceptibility zones of study area. 39

LIST OF TABLES

Table 1. Scale for pair-wise comparison in Analytical Hierarchy Process..................19
Table 2. Random Index Proposed by Saaty for the specific number of parameters. ...19
Table 3. Factor wise pairwise comparison matrix for each causative factor and its sub factors...34
Table 4. Pairwise Comparison Matrix for entire causative parameters of landslides..36
Table 5. Summary of AHP of all parameters..36
Table 6. Percentage of landslide susceptible area...38
Table 7. Validation of the Landslide Susceptibility Map by using known landslide areas. 40
Table 8. Validation of Scoops 3D results using the inventory data. 43
Table 9. Comparison of the abilities of AHP and Scoops for landslide susceptibility of the study area. 48

LIST OF ABBREVIATIONS

Abbreviation	**Explanation**
CPEC	China Pakistan Economic Corridor
GIS	Geographic Information System
AHP	Analytic Hierarchical Process
WLC	Weighted Linear Combination
KKH	Karakoram Highway
RI	Random Index
GHG	Green House Gas
AFOLU	Agriculture, Forestry and Other Land Uses

ABSTRACT

Landslides is considered as the most dangerous natural hazards in the mountainous region caused by deforestation, heavy rainfall and earthquake. The objectives of this study were to map the deforestation and use an Analytical Hierarchy Process (AHP) along with Weighted Linear Combination and Scoops 3D model to map the Landslides susceptible areas along the Karakoram Highway (KKH). The study area includes a part of Karakoram Highway which is included in the China-Pakistan Economic Corridor (CPEC) within Pakistan. This research incorporated the geomatics techniques for monitoring the forest cover change and assessing landslide susceptibility along Karakoram Highway, Pakistan. Supervised image classification was performed in ArcMap ver. 10.5 to identify changes in the forest cover along KKH. In order to study the slope stability of the area, the Analytical Hierarchy Process along with Weighted Linear Combination and Scoops 3D was used. The causative parameters for running AHP comprises of the lithology, presence of thrust, land use land cover, precipitation, and Digital Elevation Model (DEM) derived variables (slope, curvature, aspect, and elevation). Scoops 3D model incorporated the 3D properties of subsurface and the earthquake loading data. The study used Landsat 4, 5 TM, Landsat 7 ETM and Landsat 8 OLI imagery for 1990, 2000, 2010 and 2016, respectively. The results categorized the region into five major land use land/cover classes i.e., forest, vegetation, urban, open land and snow cover. Results from post classification forest cover change maps illustrated remarkable decrease (26 %) in forest cover in the last two and a half decades. The primary cause of the forest cover dynamics is the shift of native forest towards urbanization and urban vegetation. Nonetheless, there is no significant change in the reserved forested area which makes only 2.97% of the total forest cover. The results from AHP and WLC identified four landslide susceptibility zones, i.e. low, moderate, high and extremely high susceptible zones. Almost 73% of the total area fall in moderate to high susceptible zones. The results of limit equilibrium analysis using Scoops 3D categorized the area into 4 groups of slope failures volume, i.e., low, moderate, high and extremely high mass. The validation of outputs from AHP and Scoops 3D were validated using landslides inventory produced by Geological Survey of Pakistan. The results from both the techniques showed similar output that coincides with the known landslides areas. However, Scoops 3D provide not only the susceptible zones but also the range of volume of the potential slope failures. The intense forest degradation and risk-prone topography of the studied region has amplified the risk of landslides. Henceforth, effective policies and forest management are needed to protect not only the environmental and aesthetic benefits of the forest cover of this area but also to manage the disaster risks. The results of this research will help in comprehending the deforestation and forest degradation patterns. This is expected to serve in efficient forest conservation and management plans and policies.

Chapter 1

INTRODUCTION

1.1.Background Information

Forests are essential for sustaining life on the planet Earth. It provides various goods and services including food, timber, fuelwood, and fodder. Forests are essential for the ecosystem conservation, water quality management, and maintenance, reducing and preventing natural hazards like floods, erosion, avalanches, and droughts. Hence, they help in the regulation of climate on the regional levels. Numerous socioeconomic benefits are also yielded from the forests that include employment, forest products and areas with cultural values (FAO 2006).

Ecologically, forests are of great concern for the environment especially in this industrially rich era as they play a vital role as carbon sinks and help in combatting the high levels of carbon which is critical for the mitigation of global warming (FAO 2010). There's a global decline in forest cover in the past two and a half decades. Previously, the total area of 4128 million ha was covered with forests in 1990, but by the end of 2015, the forest cover was recorded to be 3999 million ha. Therefore, global forests have suffered a decline from 31.6 % to 30.6 % (FAO 2015).

A key source of carbon emissions is forest degradation. Reduction of canopy cover and drop in quality of the forests are the common indicators of degradation. It could be as a result of official and illegal logging, overgrazing, disease, forest fire and consumption of fuelwood. It is often a complicated procedure and it carries great significance for the developing countries where programs like REDD+ are being held (Gilani et al. 2015). The Agriculture, Forestry and Other Land Uses (AFOLU) sector accounted for just under 1/4th of the total human-caused greenhouse gas (GHG) emissions. Neglecting the emissions caused by agriculture, during 2000-2009 the remainder of the sector contributed almost 12% of total GHG emissions. This is due to the growing deforestation phenomenon. Although it was surprisingly observed that some countries of Latin America had a decreasing trend in deforestation, yet the deforestation continued to be the solitary highest contributor to greenhouse gas emissions from the AFOLU sector (IPCC 2013).

With the high rate of conversion of forest cover to agricultural land and urban areas, the vulnerable regions are at high risk of the onset of landslides. The change is done to accommodate and meet the needs of the increasing population. However, little considerations are made to adopt appropriate agricultural practices which in turn makes the slopes vulnerable and more susceptible to the events of landslides. Community-based approaches and participatory efforts are encouraged to address the issue of deforestation and forest degradation (Yann le Polain and Lambin 2012), (Gilani et al. 2015).

Landslide susceptibility is termed as the “the tendency of the slope/terrain to erode or disrupt and fail” (Varnes 1984; Yalcin 2008; Hung et al. 2016). Landslide susceptibility mapping is a strategic process of ranking the regions into the various degree of potential slope failures by the integration of the causative factors. The selection of causative factors depends on the complex understanding of the slope features. The consistency of landslide susceptibility zonation primarily relies on the availability of data, the scale of research and the methodology implied for the analysis and modeling of slope failures (Fell et al. 2008; Daneshvar 2014). Landslide susceptible mapping offers a baseline and simple tool for geologists, engineers, environmentalists, and land use planners by aiding them in their respective mitigation, restoration and development plans (Feizizadeh et al. 2013). Landslide susceptibility mapping has been widely implied in research for about 4.5 decades (Nilsen 1979; Wagner et al. 1988; Brabb 1993; Nagarajan et al. 2000; Colombo et al. 2005; Intarawichian and Dasananda 2010; Kanwal et al. 2017). Researchers have been applying integrated approaches to map the spatial distribution of landslide events and how the environmental parameters influence their occurrence. Geographic Information System and Remote Sensing are advanced technologies that are used in conjunction with the available data to study the hazards and impact of these events. GIS and remote sensing technology provide accurate and refined spatial models to study the environmental phenomenon like landslides hazard zonation (Gorsevski et al. 2006). The literature about landslide risk assessment reveals various GIS-based methodologies that can be broadly categorized as qualitative and quantitative approaches. The quantitative approach comprises of Analytical Hierarchy Process (Ayalew et al. 2005; Yalcin 2008; Mondal and Maiti 2012; Mashhadifarahani 2015; Basa et al. 2016), Fuzzy logic approach(Champatiray 2000; Saboya Jr et al. 2006), logistic regression (Guzzetti et al. 1999; Ayalew et al. 2005; Chang and Chiang 2009; Xu et al. 2012), multivariate statistical models (Kanungo et al. 2012), artificial neural network approach (Ercanoglu 2005; Pradhan and Lee 2010) and weighted overlay methods (Cardinali et al. 2002; Ayalew et al. 2004; Preuth et al. 2010). The qualitative approach usually combines the expert knowledge to monitor the geomorphological and geological features prone to slope failures. Typically, the qualitative approach relies on the integration of weights and ranks derived from quantitative approaches (Ayalew et al. 2005). Various models incorporate triggering factors - rainfall-induced landslides models include SHALTSAB and TRIGRS (Sorbino et al. 2010), and earthquake-induced landslides models include rigorous Newmark sliding block model(Newmark 1965; Jibson and Jibson 2003) and Coupled stick-slip deformable sliding block model(Travasarou et al. 2003). Empirical methods for landslides run out analysis involves the assessment of travel distance of mud and rock that turns in debris slides and debris flows (Duncan and Wright 1980; Hungr et al. 1989; Cannon 1993; Fannin and Wise 2001).

The three parameters that are frequently being used as the indicators of forest degradation are as follows (Lund 2002):

- The decrease in biomass attributed to reduced canopy cover and the frequency of trees per unit area.
- Reduced biodiversity- the amount of dominant and non-dominant species, number of habitats and a specific number of present species.
- Changes in quality of soil, as shown by soil fertility, soil depth, soil cover.

The GIS techniques were used to identify the forest degradation in Pakistan. (Ali T et al. 2006; Raza et al. 2012)

Landslides due to deforestation are a constant issue in mountainous areas. The roots of the trees are responsible for a firm structure on the slopes of hills. The roots provide strength to the soil by frequently piercing the bedrock. After the removal of the trees, the soil is exposed hence results in weak slope causing soil erosion. This renders the soil susceptible for landslides. Researchers have revealed that such weak slopes are 2.8 times more prone to cause landslides than the forested regions (Haigh 1984). Impact of vegetation on the slope stability should be considered in the following ways:

- Infiltration is reduced due to the loss of water from absorption and evaporation.
- The shear strength is increased as the roots reinforce the soil.
- Porewater pressure is reduced as the roots absorb the water from soil for carrying out transpiration.
- Roots anchor the soil into the firm and stable layers in order to give support and strength to the slope.
- Soil particles on the ground and roots beneath it prevent their susceptibility to soil erosion.

In order to formulate a strategic plan and mitigation measures for landslides, it is necessary to identify, categorize, assess and delineate susceptible areas for landslide hazards(Pan et al. 2008).

1.2.Rationale

According to the international standards, the estimated area for a country to be covered with forests should be 25%. Unfortunately, Pakistan falls too short of this standard and has only about 4.8% of its land covered with forests. Therefore, the current study aims to focus on the Karakoram Highway since the region is blessed with some of the great forest reserves, it is a strong motivation to assess the forest degradation. The fact that this highway runs along the region with high topographic relief and is prone to soil erosion makes it susceptible to landslides. Moreover, the general shift towards urbanization and agricultural practices gives the incentive to analyze the slope instability and landslide susceptibility (Rashid B and Iqbal 2018).

1.3. Objectives

1) To monitor and map the temporal changes in the forest cover along the Karakoram Highway from 1990's to 2016.
2) To map the landslide susceptibility zones due to deforestation and other factors using the AHP technique
3) To analyze the slope instability and identify landslide susceptibility zones using Scoops Model
4) To compare AHP and Scoops capabilities for landslide zonation.

1.4.The scope of the study

The study area is included in China Pakistan Economic Corridor (CPEC) which is a framework of regional connectivity. KKH is not only intended to benefit Pakistan and China, but it will also be beneficial to the neighboring countries; Afghanistan, Iran, India, and the Central Asian Republic region. It is a step towards economic regionalization in this globalized world. Hence, due to its enormous economic significance and high topographic relief, it makes high motivation for monitoring landslide susceptible zones (Rashid B and Iqbal 2018). Landslide mapping of this region is an essential and urgent task for the government to formulate and promote effective strategies in land use planning and sustainable development and also welcome the economic advancements from the neighboring countries. Numerous studies on landslide susceptibility mapping have been performed in the cities that are situated near the highway and incorporated complex causative factors (Basa et al. 2016; Kanwal et al. 2017). However, this study will identify the landslide susceptible areas along Karakoram Highway from Hasanabdal to Chilas and also provide a comparative account of the landslide susceptibility models, i.e. Scoops 3D and Analytical Hierarchy Process.

Chapter 2

MATERIALS AND METHODS

2.1. Study Area

The Karakoram Highway (KKH) is among the highest international highways. It is at an altitude of 4,693 m or 15,397 ft. The total length of KKH is about 1300 km, and it stretches approximately 700kms from Islamabad through Karakoram Mountains into China. Along the path, there are some of the high mountain ranges like Pamirs, Himalayas, and Karakorams. Huge barren mountains dominate majority of the highway. Indus River runs through KKH for over 200 km. The Karakoram Highway along with Indus River divides the mountain range of the Himalayas and Karakoram Range and winds along the foot of Nanga Parbat. KKH leaves the Indus for Hunza, Gilgit and Khunjerab River to take to Karakoram Range. As the road extends till Khunjerab Pass, it crosses the Central Asian Plateau before winding down through Pamirs to Chinese City of Kashgar, along with the western side of Taklamakan Desert (Rashid B and Iqbal 2018).

The study area lies between the latitude of 33^o and 35^o (N) and longitude from 72^o and 73^o (E) (figure 1). The current study area covers the Karakoram Highway (N35) originating from Hasanabdal to Sazin region. Some of the dense forest reserves are located along this highway. The highway runs along high topographic relief area and is at risk of soil erosion. This makes for an excellent incentive to identify the landslide susceptible zones.

Physiography

The Karakoram Highway (KKH) is included in the highest international highways. Karakoram Highway lies at an altitude of 4,693 m or 15,397 ft. The entire length of the highway is around 1300 km, and it stretches approximately 700 km from Islamabad through Karakoram Mountains into China. The study area for this research comprises of Hasanabdal to Sazin. Along the highway, some of the beautiful mountain peaks such as Pamirs, Himalayas, and Karakorams can be observed. Vast barren mountains characterize most of the highway. Indus River goes parallel with KKH for about 200 km. The KKH along with Indus River splits the mountain range of the Himalayas and Karakoram Range and winds along the foot of Nanga Parbat. KKH leaves the Indus for Hunza, Gilgit and Khunjerab River to take to Karakoram Range. As the road extends till Khunjerab Pass, it crosses the Central Asian Plateau before winding down through Pamirs to the Chinese City of Kashgar, along with the western side of Taklamakan Desert.

Climate

The KKH runs along some of the great tourist attractions of northern areas of Pakistan. Usually, the study area observes mild summers and extreme winters with snowfall. The annual precipitation ranges from 150 mm to 2000 mm. The maximum annual average temperature ranges from 16^{o} to 25^{o} C and minimum annual average temperature range is between 3^{o} to 14^{o} C. The precipitation pattern of the study area is illustrated in the Figure 5c.

Geology and Soil Composition

Lithology is generally considered to be one of the significant factors for causing landslides. Different rock types and composition have specific mechanical strength. Fragile rocks with foliated and sheared surfaces are more susceptible to landslides. The lithology map is generated using the road log (1: 250,000) of KKH. The various types of minerals and chemical composition of the area defined in Appendix 1 and the lithology map is shown in Figure 5b.

2.2. Dataset Used

In the identification of forest cover change, acquisition of satellite imagery is the first step. Whereas in the landslide susceptibility mapping, the first and foremost step is to identify the causative factors for the landslides incidents. In order to identify the landslide susceptibility zones, the factors should be consistent, readily available and illustrative. The leading cause for triggering landslide events is the slope failure. Several other factors such as precipitation, land cover and drainage also influence landslides. Hence, a total of 7 landslide constraints are used in this research.

The main landslides causative parameter such as slope, elevation, aspect, curvature, precipitation, lithology and landcover are incorporated for the landslide hazard assessment. The factors are grouped into four main categories. The first category is the human-induced factor that comprises of the land cover map, the meteorological group with precipitation information map, the topographic data that contains lithology layer and proximity to MMT and the last set of factors is derived from Digital Elevation Model (DEM) that contains Slope, Aspect, Elevation and Plan Curvature.

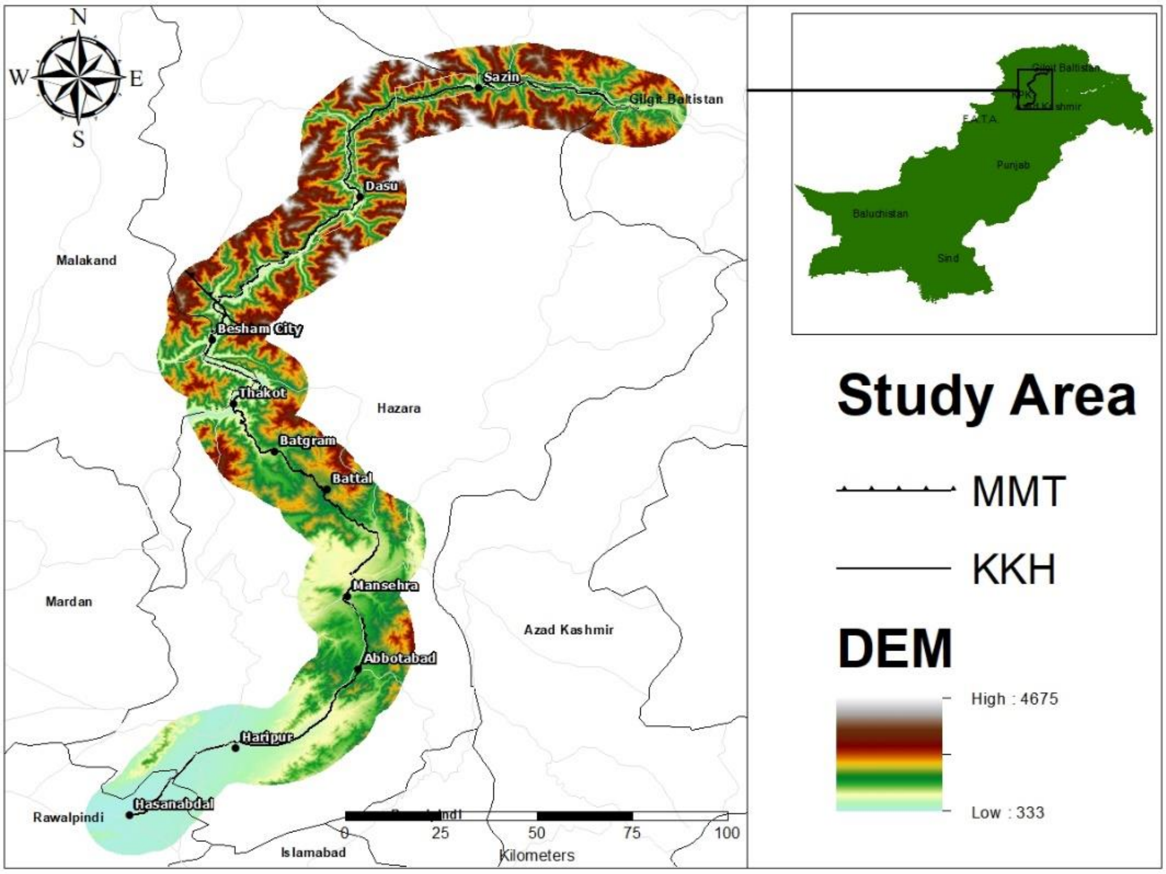

Figure 1. Study area map of Karakoram Highway (N-35) from Hasanabdal to Sazin.

.

Satellite Images

Landsat remote sensing program started in 1972 by the launch of its first satellite, Landsat 1 and the latest functioning satellite is Landsat 8. Over the years, the Landsat image resolution has been improved by the addition of 2 additional spectral bands (Band 1 and 9) thus giving much-detailed information in the Landsat 8.

For this study, the 30-m satellite imagery (less than 10% cloud cover) for the years 1990, 2000, 2010 and 2016 were attained from Landsat 5 and 8. The images were taken from the summer season (June through September). These raw images were initially preprocessed, mosaicked together and clipped to extract the required region (Rashid A 2004).

Digital Elevation Model(DEM)

DEM of 30 m spatial resolution was acquired from SRTM website. The DEM has been registered w.r.t WGS 1984 UTM Zone 43 system. The shapefile of the study area with 10 km buffer was utilized to clip the DEM. The DEM was then processed using ArcGIS 10.5 by using the HEC-HMS Module. This was so done to get a depression less DEM in order to generate the landslide causative parameters, slope, elevation, aspect and plan curvature.

Geological Map

The lithological map was generated after digitization of road log (geological map) of scale 1:250,000 km acquired by the Geological Survey of Pakistan (GSP).

Precipitation Map

The rainfall data from 9 neighboring meteorological stations of Balakot, Bunji, Astor, Mallamjabba, Dir, Kakul, Gilgit, Risalpur and Skardu was acquired from Pakistan Meteorological Department, Islamabad.

2.3. Software Used

The GIS software used for this study include ArcGIS ver 10.5, ERDAS IMAGINE ver 2014 and Scoops 3D. The other software used include Microsoft Office (Word, Excel and PowerPoint).

2.4. Methodology

The entire methodology of the current study is illustrated in Figure 2.

2.4.1. Forest Cover Change Mapping

The methodology flowchart for forest cover change mapping is shown in Figure 3. Image classification of the land cover includes allocating pixels to the classes which give the information about the land use. It represents the piece of land used for various purposes such as forests, urban areas, agriculture, etc. Land use land cover classification is an integral component of remote sensing and has been utilized in several analyses including change detection, urbanization research, etc. Image classification is mainly divided into two main groups; per-pixel based and object-based classification. Per-pixel based image classification is mostly commonly used in the researches.

In this study, forest cover change was assessed using the per-pixel based supervised image classification is performed. The classification was performed using the following three steps:

1. Selecting the training sites
2. Evaluating training samples by their signatures and spectral patterns.
3. Image classification.

For each land cover class, approx. 20-30 samples were selected as the training sites. Supervised Image Classification is performed in ERDAS IMAGINE.2014. Following classes are identified on the satellite images:

Urban: Includes urban settlements and arrangements like roads and houses

Vegetation: Consists of the urban vegetation such as green belts, recreational parks, and the agricultural fields

Open Land: Barren mountains and areas with no vegetation

Forests: Areas covered with dense trees and the reserved forests

Water: Water bodies including the Indus River and streams.

Snow: Snow cover

Accuracy Assessment

The interpretation of the images is performed visually and is reinforced by the image classification. Accuracy assessment is a fundamental part of the classification. The concept is to compare the classification results to other data source which is deemed to be more accurate or using the ground truth data.

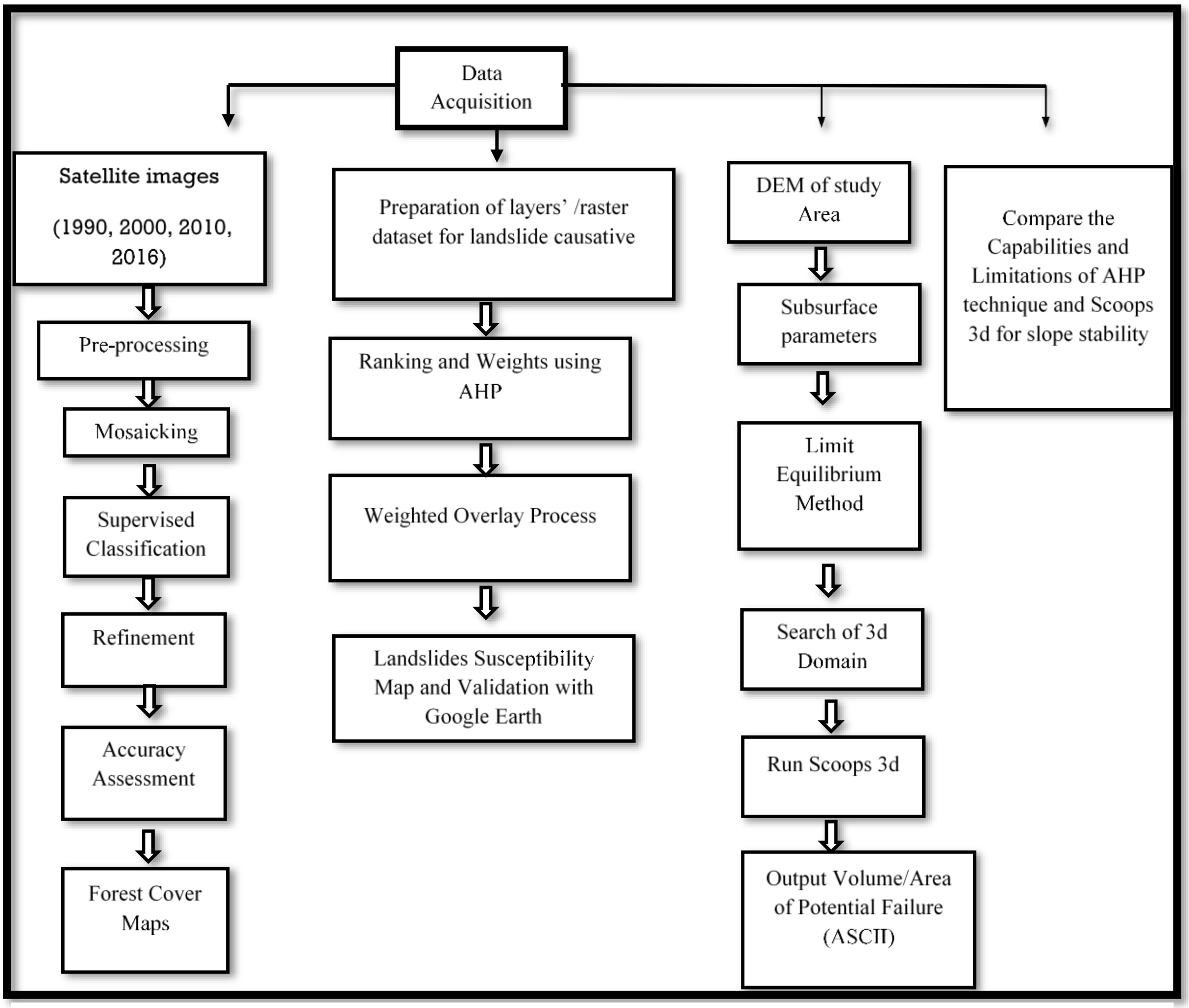

Figure 2. Complete work flow chart for the identification of forest cover dynamics and landslide mapping.

Ground truth can be performed in the field; however, it is not preferred because it is an expensive and time-consuming process. Ground truth data can be generated from the interpretation of high res image, current classified imagery or the GIS layers.

Accuracy assessment for the classified images is performed in ArcGIS using three geoprocessing tools: Create Accuracy Assessment Points, Update Accuracy Assessment Points, and Compute Confusion Matrix. The accuracy assessment is a 2-step process; in the first step, a set of random points were generated from the ground truth data, and in the next step these are compared to the classified data in the confusion matrix. In the current study, Google Earth is used as the reference data for accuracy assessment.

2.4.2. Landslide Susceptibility Methodology

The procedures of the Analytical Hierarchy Process (AHP) and Weighted Linear Combination (WLC) was utilized to generate the landslide susceptibility map. Causative parameters/ maps are incorporated using remote sensing data and GIS layers. The complete flowchart for the landslide susceptibility is shown in Figure 4.

Data is gathered from various sources ranging from satellite imagery, GIS layers, and tabular data. Some parameters like slope, elevation, curvature, and aspect are extracted using the Digital Elevation Model. Digitized vector layers are converted into raster format for analysis in ArcGIS. The causative factor maps are of 30 by 30-meter resolution. After the data preparation, AHP and pairwise comparison matrix are calculated for developing Landslide Susceptibility Index (LSI). LSI values are then grouped into four landslide susceptible zones in ArcGIS to generate a landslide susceptible map of KKH (Hasanabdal to Sazin). The classes are (a) extremely high, (b) high, (c) moderate and (d) low.

Analytical Hierarchy Process

Saaty introduced the AHP technique in 1980. The Analytical Hierarchical Process is used to compare the causative factors of landslides. By incorporating the professional expertise and literature review, the weights for all the parameters are assigned. In order to create a pairwise comparison matrix, a relative value range from 1 to 9 is assigned, and each factor is given value against the other factor in the cell. If the factor in the vertical array is strongly significant than the one in a horizontal array, then the values range from 1 and 9. Contrarywise, the reciprocal values ranging from ½ to 1/9 is of landslides (Ladas et al. 2007).

A scale proposed by Saaty (Table. 2) is used to assign the preference values for the landslide causative factors. A pairwise comparison matrix for the factors is computed using the preferences thus weights for each factor is calculated.

Consistency Ratio (CR) is calculated using the following formula:

$$CR = CI/RI \qquad \text{Equation (I)}$$

Where

CI= (λ-n)/n-1

Λ= Average consistency vector

n= Number of factors

Saaty presented the Random Index (RI) that depends on the number of factors (n) as shown in Table 3.

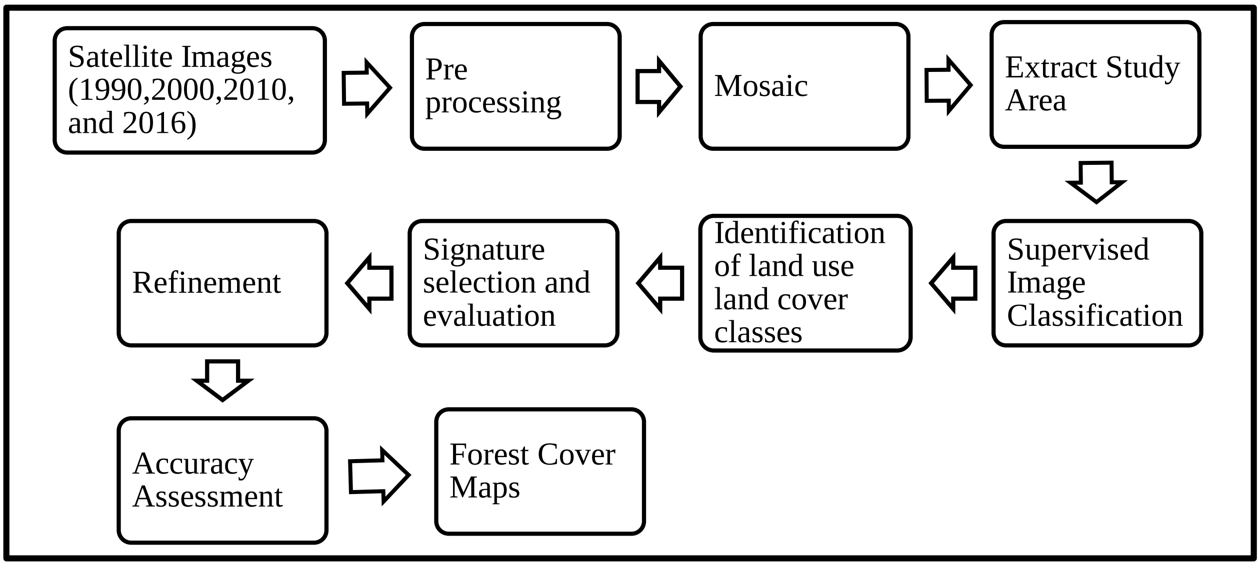

Figure 3. Flowchart for mapping the forest cover dynamics from 1990 to 2016.

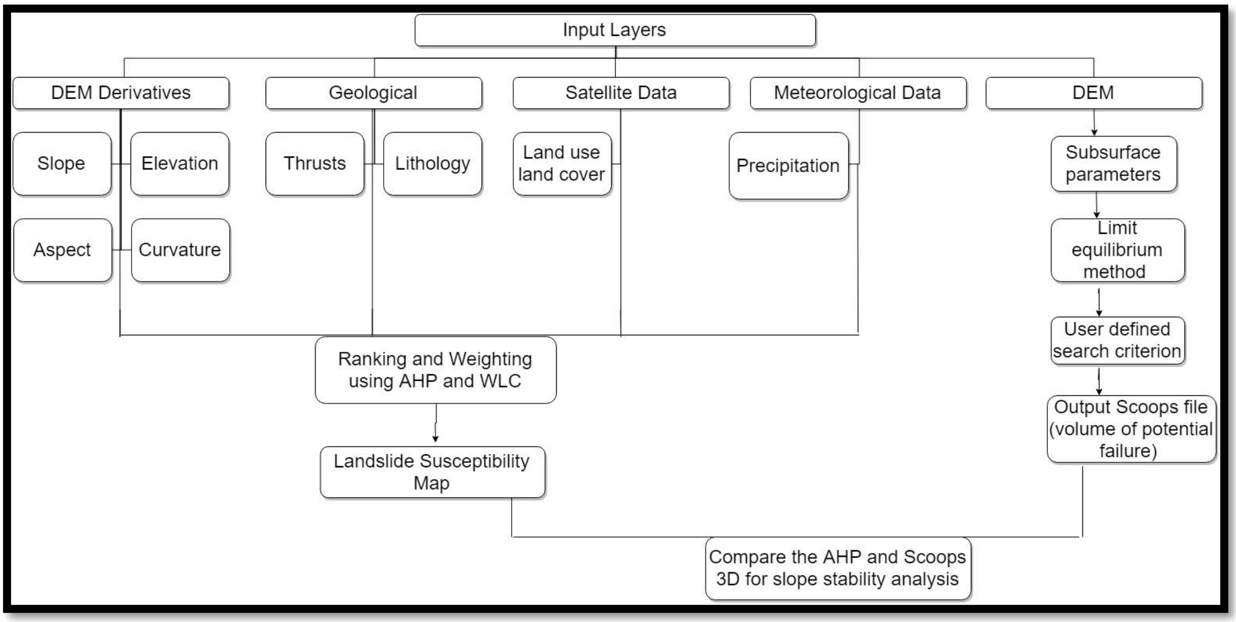

Figure 4. Landslide susceptibility mapping through AHP and Scoops model.

Table 1. Scale for pair-wise comparison in Analytical Hierarchy Process.

Intensity of importance	**Definition**
1	Equal Importance
2	Equal to moderate importance
3	Moderate importance
4	Moderate to the strong importance
5	Strong importance
6	Strong to the very strong importance
7	Very strong importance
8	Very strong to the extremely strong importance
9	Extreme importance

Table 2. Random Index Proposed by Saaty for the specific number of parameters.

RI					
n	**RI**	**n**	**RI**	**n**	**RI**
1	0.00	**6**	1.24	**11**	1.51
2	0.00	**7**	1.32	**12**	1.48
3	0.58	**8**	1.41	**13**	1.56
4	0.90	**9**	1.45	**14**	1.57
5	1.12	**10**	1.49	**15**	1.59

Weighted Linear Combination

It was developed on the weighted average in order to organize the factors and normalize them. After the standardization of factors, weights of the factor classes are combined to calculate the Landslide Susceptibility Index (LSI). LSI values are categorized into 4 landslide susceptible zones in ArcGIS 10l.5 by natural breaks to generate landslide susceptible map of the study area. The classes are (a) extremely high, (b) high, (c) moderate and (d) low. Google Earth imagery and GSP map are used for visual interpretation to generate a map of inventory of the study area. The precision of the ensuing map is evaluated by superimposing the current map on the landslide susceptibility map.

The flowchart of a methodology for landslide susceptibility map is shown in Figure 5.

Scoops 3D

Scoops 3D is software developed by United States Geological Survey (USGS) for slope stability analysis using the digital elevation model (DEM). This program systematically examines the DEM and then calculate the stability of several 3D potential landslide sites with varying range of depth and volume of the potential failures within the range of DEM **(**Reid et al. 2015**)**. The Scoops 3D uses the "method of columns" for limit equilibrium analysis to calculate the potential failures with rotational slip surface. The result is given in the form of either area or volume of the potential slope failures (landslides) which can then be visualized in any GIS or mapping software. The program has been developed in Fortran 90 programming language to ensure rapid computation and on-the-fly distribution of computer memory for various problem ranges. It's a computationally more effective method than executing the geotechnical calculations in a GIS environment. Scoops 3D works on either Ordinary (Fellenious) or Bishop's Simplified (Duncan and Wright 1980) limit equilibrium methods to assess the slope stability of the trial surfaces. Ordinary method doesn't use the iterative processing to calculate the trial surfaces and it always calculates the factor of safety (F) value for specific rotational trial surfaces. The factor of safety (F) values assessed by Ordinary method in 3D are typically lesser than the ones calculated using other limit equilibrium techniques (Lam and Fredlund 1993). However, Scoops 3D gives more accurate F values with high pore pressure (Lei et al. 2011**)**. Bishop's method uses iterative processing to calculate F values and is considered similar to more rigorous stability methods in both 2D (Duncan and Wright 1980) and in 3D **(**Hungr et al. 1989; Lam and Fredlund 1993).

Bishop's 2D simplified slices limit equilibrium method was extended into 3D method of columns **(**A.W. 1955; Hungr et al. 1989). For this method to work, it is assumed that the shear strength s, on the trial surfaces is dependent on the linear Coulomb-Terzaghi failure rules:

$$\boldsymbol{s = c + (\sigma_n - u)tan\phi} \qquad \text{Equation (II)}$$

where,

c= cohesion,

ϕ= the angle of internal friction,

σ_n = normal stress and

u = pore water pressure acting on the shear surface.

A geotechnical based analysis incorporates cohesion and angle of friction according to the subsurface properties of the area.

Using Scoops 3D (Reid et al. 2000), orthogonal grid search of grid points directly above the DEM. Individual search point of the grid is the centroid of the potential failures spheres. The intersection of the grid points and the potential failures spheres within the given radius. The factor of safety F is calculated when the intersection creates a potential failures mass within the specified volume range

This method is ideal for the potentially huge landslides by incorporating regional groundwater properties and material strengths instead of local heterogeneities in the material strengths and the hydraulic properties. This technique can also differentiate between shallow landslides and deep-seated landslides. For the current analysis, the volume of potential masses is categorized into four groups; low potential failure mass, moderate failure mass, and high and extremely high potential failure mass. In the 1st category, the landslides comprise of shallow failures and debris or mudflow. Moderate failure is an intermediate potential sliding case whereas massive mass failure consists of relatively higher and in-depth sliding material. This type of landslide is triggered due to the shaking of subsurface materials or earthquake-induced case. The seismic loading for the current study was taken from the literature (Waseem et al. 2013; Mahmood 2016). The shear strength values were assigned by the shear strength properties of the lithology of the shallow landslides. Unit weights were assigned on the base of the finite element limit equilibrium analysis.

Chapter 3

RESULTS AND DISCUSSIONS

3.1. Forest Cover Change

The maps for forest cover of the area and the results of error matrix and kappa coefficients were calculated for the years 1990, 2000, 2010, and 2016 (Fig 6). The overall accuracies for the classification of 1990, 2000, 2010 and 2016 are 88%, 85%, 83% and 89% with the kappa coefficients 0.83, 0.78, 0.77, and 0.85 respectively. The percentage change in each class of land cover is summarized in Figure 5. The results demonstrated a radical reduction in forest cover and consequent growth in the urban areas (10 %) and vegetation (38 %). Previously, 46 % of the total study area was covered with forest in 1990 which has been significantly decreased to only 20 % in 2016. These results showed that about 26 % of forested land had been degraded in the last two and a half decades (Rashid B and Iqbal 2018).

The study area is predominantly populated with conifers and pine forests. The forest types along KKH comprise of the subtropical pine forest, Himalayan moist temperate forest, Himalayan dry temperate forest, and subalpine forests. Chir Pine (Pinus roxburghi) are the dominant forest species found at an altitude of 900 m to 1700 m. Whereas the major conifer species in the order of higher elevation comprise of the Cedrus dedora (Deodar, diar), Picea smithiana, Pinus wallichiana and Abies pindrow (Partal) (Siddiqui 1997). However, no substantial shortage in the reserved forest was found which almost cover 2.9 % of the total cover. If the deforestation followed the same unsustainable pattern, the forest species in the study area are expected to go endangered (Rashid & Iqbal 2018).

The primary reason for deforestation in the study area comprises of continuous and every growing demand for wood and area shift to pastures and parklands. The area displayed a drastic increase in the agricultural and aesthetic vegetation. This vegetation type is also exposed to high grazing. Wood consumption for domestic purposes and village carpentry also contributes to the forest degradation in the study area (Siddiqui 1997). Several reports relate deforestation with its connection to timber mafia and competitor groups for financial benefits and clearing by security forces for strategic reasons (Ali T et al. 2006; Fischer et al. 2010; Rashid B and Iqbal 2018).

The deforestation drivers in the study area include consumption of fuelwood, the trend towards urbanization and also the timber mafia. As far as the natural cause of deforestation is concerned, the mountainous region of Pakistan has not observed any major forest decline due to environmental factors like climate, water, epidemic or landslides, etc. However, due to the ongoing consumption of trees for fuelwood, the forests of Hazara and Malakand may become extinct by the year 2027. In these areas, around 21 % of the total demand is covered by rangelands, plantation and agricultural supplies. The demand/supply gap is currently approximately 8.8 million m^3 that is likely to keep increasing up to 13.6 million m^3 by the year 2050 (Haeusler et al. 2000). Nevertheless, the mountainous areas of the country still haven’t observed any major forest decline due to natural and environmental factors such as water, epidemic, climate or landslides, etc (Rashid B and Iqbal 2018).

If the deforestation pattern continued, the biodiversity of the area would be endangered, and it will also have an adverse impact on the ecosystem services both recreational and aesthetic facility, soil conservation and carbon sequestration. Removing the vegetation from steep slopes make the area susceptible to erosion and other natural hazards and disasters such as landslides (Hamilton 2008). The Himalayan region carries immense importance in this aspect because any damage to this region will have a negative impact on this region but also on the adjacent Indus plains via hydrological cycle. This may trigger the onset of soil erosion, floods, silting and desertification. The floods are more frequent and intense hazard in the last two and a half decades relative to the past 65 years due to the increased rate in surface runoff and soil erosion the region (Tejwani 1987). According to Pakistan Water Strategy, Pakistan is expected to have even more water storage of 18- million acre-feet (MAF) by the year 2050, out of this 30 % is to replace storage loss because of silting (Qamer et al. 2016) (Rashid B and Iqbal 2018)

3.2. Landslide Susceptibility Mapping Using AHP and WLC

Causative Layer Preparation

1. **Elevation**

The elevation and landslides are not directly related. Although the elevation does not play an active part in the onset of landslides, however, its influence in hazard assessment cannot be neglected. Values of elevation (334-4690m) are distributed in 5 classes according to natural breaks (Jenks): (i) 334-863 m (ii) 863- 1478m (iii) 1478-2127 m (iv) 2127- 2896 and (v) 2896- 4690m. Elevation map is shown in Figure 1.

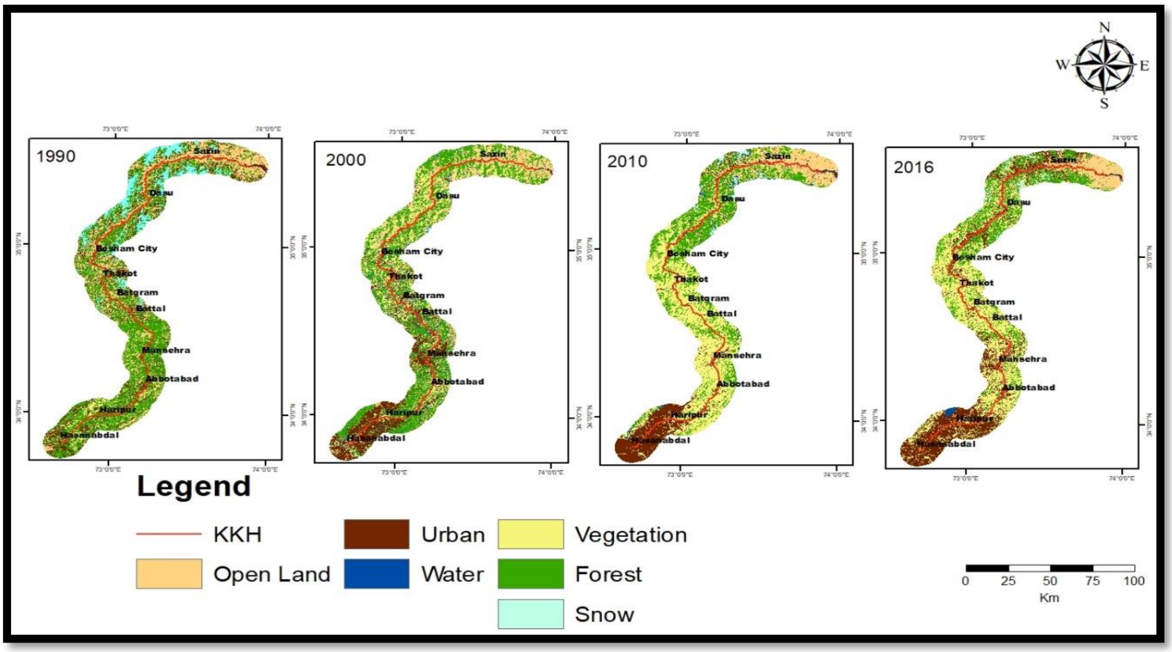

Figure 5. Forest cover dynamics along KKH from 1990 to 2016.

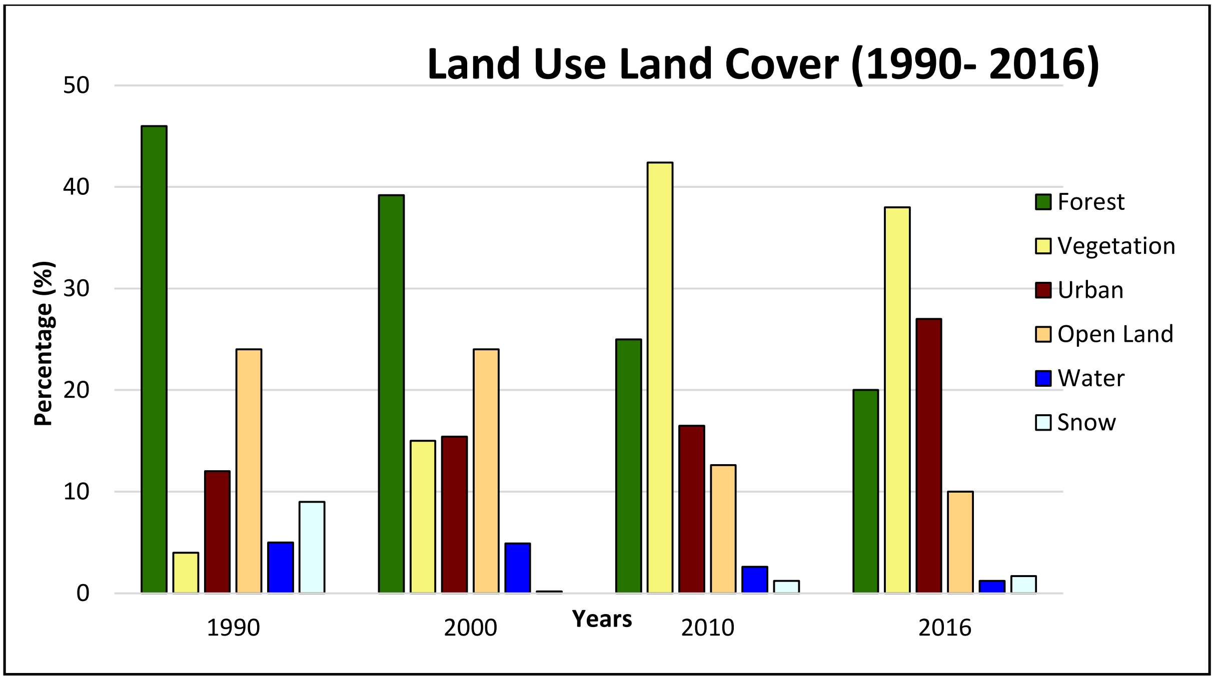

Figure 6. Spatiotemporal change of each LULC class from 1990 to 2016.

Forest Cover Change (decrease in area %) = 46%- 20%

= 26 %

2. Slope Degree

The slope is considered to be the most significant contributing factor for the landslides. The slope governs other critical influencing parameters like the type and extent of vegetation, soil water content, and precipitation of a particular area. In general, higher slope angles indicate more susceptibility to landslides. Slope gradient affects the velocity and time taken for the subsurface drift after the rainfalls. Higher slope gradient also causes an increase in the shear strain in the unstable soil cover. The slope map is derived used the SRTM 30-m DEM. The slope of the study area varies from 0^{o} to 89^{o}. The slope values are classified into three major groups; (i) gentle slope (0 to 30), (ii) Moderate to steep slopes (30 to 60) and (iii) >60 that comprises of cliffs and escarpments. Generally, landslides do not occur on the gentle slopes. Landslide-prone areas have sharp gradients reflecting the most in the 2^{nd} class. Slope map of the study area is shown in Figure 7a.

3. Lithology Map

Lithology is observed to be one of the significant factors for causing landslides. Different rock types and composition have specific mechanical strength. Fragile rocks with foliated and sheared surfaces are more susceptible to landslides. The lithology map is generated using the road log (1: 250,000) of KKH. The proximity to MMT is also a key factor in the landslide susceptibility mapping, so the buffers of 200 m, 500 m and 700 m around the Main Mantle Thrust was created to see the impact of active thrust to the neighboring areas. The Figure 7b illustrates the lithological composition of the study area.

4. Precipitation Map

Precipitation is a chief causative factor for landslides. Monthly rainfall data is acquired from the meteorological stations of Astor, Bunji, Balakot, Gilgit, Mallamjabba, Dir, Risalpur, Kakul and Skardu. Using the precipitation data, annual precipitation map is generated using the Inverse Distance Weighted (IDW) interpolation techniques. The study area experienced 246 mm to 1328 mm annual rainfall in the last 2.5 decades (1990-2014). The precipitation map for the study area is represented in Figure 7c

5. LULC Map

The LULC Map was generated using supervised image classification. Theoretically, barren land is prone to landslides as compared to other lands. The fact that there is no root to withhold the soil in its position.

On the contrary, forested areas have deep roots to restrict the landslide incidents. This soil provides mechanical and hydrological strength and stability to avoid soil erosion and thus prevent the occurrences of landslides. Moreover, the forest cover change for agriculture purposes or using unsuitable cropping techniques can increase landslide susceptibility. The LULC map is shown in Figure 7d.

6. Plan Curvature

Plan curvature represents the geomorphological pattern of the topography of any area. This is chosen as inducing parameter as it affects the hydrological features of soil and surface erodibility by influencing the runoff flow down the slope. This is either calculated as plan curvature, common curvature or profile curvature. The flat surface is indicated by a 0 whereas positive values indicate convex surface and negative values indicate concave surfaces. Low lying areas are represented with 0 to lower positive and lower negative values. Since zero signifies flat surface, so it has the lowest susceptibility to landslides. Concave surfaces have a relatively higher susceptibility to landslides as compared to convex slopes. After the rainfall occurs, concave slope retains more water and for a longer period. For the current study, the curvature map was generated using the DEM. The curvature indicated three classes the flat, the concave surfaces and the convex surfaces as shown in Figure 7e

7. Aspect Map

Aspect is studied as a landslide inducing factor in monitoring the landslide susceptibility zones. Aspect is the sunlight reflection, drying winds and precipitation which further influences other factors like evapotranspiration and saturation levels of the slope gradient and soil loss. Hence this factor is responsible for soil erodibility and unsymmetrical slope deterioration which is why it is categorized in 9 classes: flat (-1), north (0 – 22.5), northeast (22.5 – 67.5), east (67.5- 112.5), south-east (112.5 - 157.5),south(157.5 – 202.5), south-west (202.5 – 247.5), west(247.5 -292.5), northwest(292.5 – 337.5) and north (337.5 -360) as illustrated in Figure 7f. As per the literature (Rashid A 2004), the southwest to southeast Monsoon rainfall has a significant impact on the slopes in the south to northwest direction. Hence, the slopes towards the south-west are more susceptible to landslides and then comes the northwest region.

Analytical Hierarchy Process and Weighted Linear Combination

The analytical Hierarchical Process (AHP) is a multi-criterion decision based process model which was proposed by Thomas L. Saaty (Saaty 1980) AHP is considered one of the most accurate and authentic methods to expedite effective decision making by incorporating empirical data and subjective knowledge of the planners and decision makers (Şener et al. 2011). The AHP runs according to the 9-point scale to rank the relative preference of each criterion against the other (Saaty and Vargas 2000).

Therefore, AHP and normalization of the results of the pairwise comparison matrix, various weights were assigned to each factor/ parameter concerning its potential level of landslides susceptibility. This is a logical and organized way to create weights for the heuristic weighted overlay technique and elude inconsistencies within the weights.

The pairwise comparison matrix for the eight causative parameters for each parameter class is listed in table 4. The values of the comparison matric are the expert knowledge and the literature evidence that supports the significance and preference of each parameter.

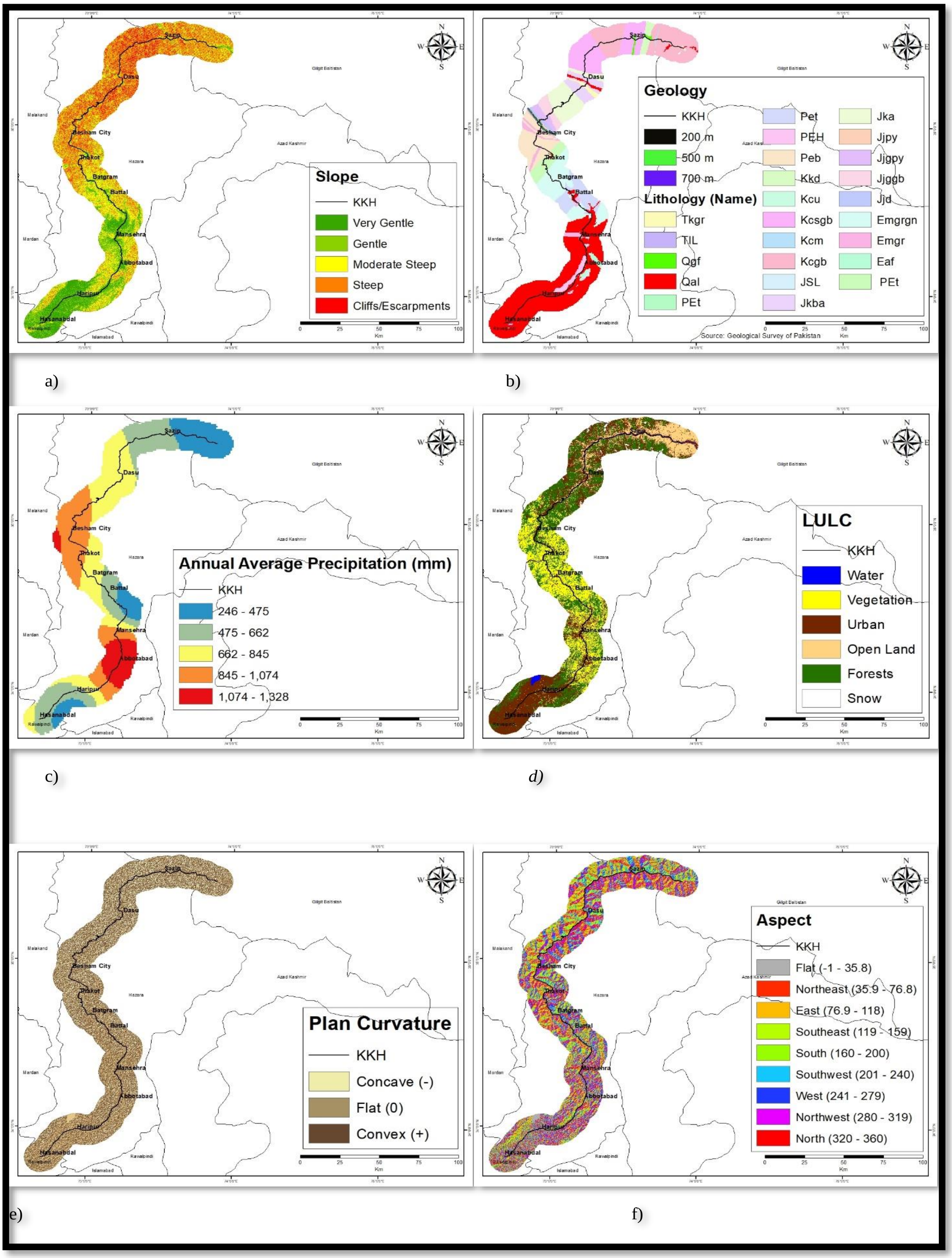

Figure 7. Causative Layers for AHP
a) Slope degrees, b) Lithology and the proximity, c) Precipitation, d) LULC, e) Plan Curvature and f) Aspect.

The AHP is a general methodology proposed by Saaty (Saaty 1980) however, the ranking by the pairwise comparison matrix is performed according to the common environmental and climatic settings of the respective cities lying along the area under study. The reliability of these factors and their weights are assessed by taking eigenvectors of the pairwise matrix thereby calculating the consistency index and consistency ratios. The pairwise comparison matrix for each parameter showed that the CR values ranged between 0.001 to 0.008, which are an acceptable range. The empirical results of AHP showed that slope is the major contributing factor of landslides followed by lithology, precipitation and land use land cover. Whereas, the factors; curvature, aspect, and elevation have a lower influence with the weights 0.007, 0.002 and 0.002, respectively. The consistency ratio (CR) among the eight causative parameters is 0.068 which is a reliable value. Hence, the CR values verify and affirm the preferences are making the results reliable. This value indicates the comparison of these causative parameters are consistent and applicable to be utilized subsequently in the landslides susceptibility analysis.

Landslide hazard zonation is performed using the pairwise comparison matrix, and the weighted linear combination (WLC) of the causative parameters is achieved. A WLC map depicting a continuous numerical scale is generated. This map represents the different level of landslide susceptibility and was broadly categorized into four groups; low susceptible, moderately susceptible, highly susceptible and extremely high susceptible zones. To assess the accuracy, the qualitative approach was taken to confirm the landslide susceptibility mapping technique. The Analytical Hierarchy Process and Weighted Linear Combination based landslide susceptibility map suggests that 40 % of the total area comprises of the high susceptible zone and almost 7 % of the area falls in the very high susceptible zone. Due to the steep slope and geological features, the area is generally categorized as landslide hazard area, and almost 43% of the total area is considered to be in the moderate susceptible zone.

Landslides Susceptibility using Scoops 3D

The limit equilibrium analysis of the study area emphasizes the impact of high topographic relief that is the key controlling factor in the potential gradient failures. A large volume of slope failures represented destabilizing effect over several DEM nodes. Hence, the map of slope stability through Scoops 3D differs from that of AHP generate landslide map, in the sense that it also highlights the volume of the potential unstable sites. The resultant map generated by the limit equilibrium method showed that the area is generally steep and therefore, have the majority of the critical surfaces. The factor of safety or F is used here as instability factor for the analysis. By incorporating the strength properties of the homogeneous materials, the slope stability of the region with earthquake loading but no groundwater configuration was calculated. Under dry conditions, the impacts of the gravitational stress were found, and F_{min} is set to be 1.5.

Table 3. Factor wise pairwise comparison matrix for each causative factor and its sub factors.

						Class Weight	Factor Weight
Slope	**Very Gentle**	**Gentle**	**Moderately Steep**	**Steep**	**Cliffs**		**0.3**
Very Gentle	1	1/3	1/5	1/7	1/4	0.22	
Gentle	3	1	1/3	1/5	1/2	0.46	
Moderately Steep	5	3	1	1/5	3	1.22	
Steep	7	5	5	1	4	2.92	
Cliffs	4	2	1/3	1/4	1	0.69	

Lithology	**Qgf**	**Qal**		**0.25**
Qgf	1	6	1.70	
Qal	1/6	1	0.28	

Precipitation	**246-475**	**475-662**	**662-845**	**845-1074**	**1074-1328**		**0.09**
246-475	1	1/2	1/3	1/4	1/5	0.29	
475-662	2	1	1/2	1/3	1/4	0.46	
662-845	3	2	1	1/2	1/3	0.85	
845-1074	4	4	2	1	1/2	1.3	
1074-1328	5	4	3	2	1	2.90	

Distance from MMT	**200**	**500**	**700**		**0.09**
200	1	5	7	2.27	
500	1/5	1	3	0.59	
700	1/7	1/3	1	0.25	

LULC Classes	Water	Urban	Vegetation	Forest	Snow	Open Land	0.12
Water	1	3	5	7	2	7	0.38
Urban	1/3	1	3	5	3	4	0.24
Vegetation	1/5	1/3	1	3	1/5	2	0.08
Forest	1/7	1/5	1/3	1	1/5	2	0.05
Snow	1/2	1/3	5	5	1	6	0.21
Open Land (Barren Hills)	1/7	1/4	1/2	1/2	1/6	1	0.04

Curvature	Concave	Flat	Convex	0.09
Concave	1	5	7	2.27
Flat	1/5	1	3	0.59
Convex	1/7	1/3	1	0.25

Aspect	Flat	North	North East	East	South East	South	South West	West	North West	0.04
Flat	1	1/2	1/3	1/4	1/6	1/8	1/9	1/9	1/8	0.30
North	3	1	2	1/2	1/3	1/5	1/6	1/6	1/5	0.84
North East	2	1/2	1	1/2	¼	1/6	1/7	1/7	1/6	0.54
East	4	2	2	1	½	1/4	1/5	1/5	1/4	1.16
South East	6	3	4	2	1	1/2	1/3	1/3	1/2	1.96
South	8	5	6	4	2	1	1/2	1/2	1	3.11
South West	9	6	7	5	3	2	1	1	2	4.00
West	9	6	7	5	3	2	1	1	2	4.00
North West	8	5	6	4	2	1	1/2	1/2	1	3.11

Elevation	334-863	863-1478	1478-2127	2127-2896	2896-4690	0.03
334-863	1	1/2	1/3	1/4	1/5	0.06
863-1478	2	1	1/2	1/3	¼	0.10
1478-2127	3	2	1	1/2	1/3	0.16
2127-2896	4	3	2	1	½	0.26
2896-4690	5	4	3	2	1	0.42

Table 4. Pairwise Comparison Matrix for entire causative parameters of landslides.

Parameters	Elevation	Aspect	Curvature	LULC	Distance from MMT	Precipitation	Lithology	Slope	Wts
Elevation	1								0.03
Aspect	2	1							0.04
Curvature	5	4	1						0.09
LULC	6	5	2	1					0.12
Distance from MMT	6	5	1	2	1				0.08
Precipitation	7	6	4	3	2	1			0.18
Lithology	7	6	3	3	3	3	1		0.25
Slope	7	6	3	3	4	2	2	1	0.30

Table 5. Summary of AHP of all parameters.

	n	λ	CI	RI	CR	%CR
Slope	5	5.36	0.09	1.12	0.08	8
Lithology	2	2	0.02	0	0.02	2
Precipitation	5	5.43	0.1	1.12	0.09	9
Distance from MMT	3	3.06	0.04	0.58	0.068	6.8
LULC	6	6.45	0.08	1.24	0.06	6
Curvature	3	3.06	0.04	0.58	0.068	6.8
Aspect	9	9.09	0.01	1.45	0.08	8
Elevation	5	5.09	0.02	1.12	0.02	2
All factors	7	7.9	0.16	1.32	0.057	5.7

Table 7. Weighted Linear Combination Ranking for all the parameters.

Factor	Rating	Class Range	Class Rate
Slope	9	Very Gentle	2
		Gentle	4
		Moderately Steep	6
		Steep	8
		Cliffs	9
Lithology	8	Qal	7
		Qgf	9
		Kkkp	5
		Kkkgd	7
		Kkd	5
		Kcd	5
		Kcsgb	5
		Kcgb	7
		Kcm	1
		Kcu	7
		PEb	7
		PEt	5
		PEh	3
		Tkgr	5
		TII	3
		Jka	5
		Jkba	7
		Jjggb	7
		Jjpy	5
		Jjd	5
		Jjp	5
		Emgr	7
		Emgrgn	7
		Eaf	5
Precipitation	7	246-475	1
		475-662	3
		662-845	5
		845-1074	7
		1074-1328	9
Distance from MMT	6	200	7
		500	5
		700	3

LULC	6	Water Open Land Urban Forest Vegetation Snow	7 9 5 1 3 0
Aspect	5	Flat North East East South East South South West West North West North	0 3 2 4 6 8 9 9 9
Curvature	4	Concave Flat Convex	9 2 5
Elevation	1	334-863 863-1478 1478-2127 2127-2896 2896-4690	2 4 5 6 7

Table 6. Percentage of landslide susceptible area.

Group	**Landslide Zones**	**Pixels**	**%**
1	**Low**	701476	9.6
2	**Moderate**	3129201	43
3	**High**	2922893	40.2
4	**Extremely High**	516359	7

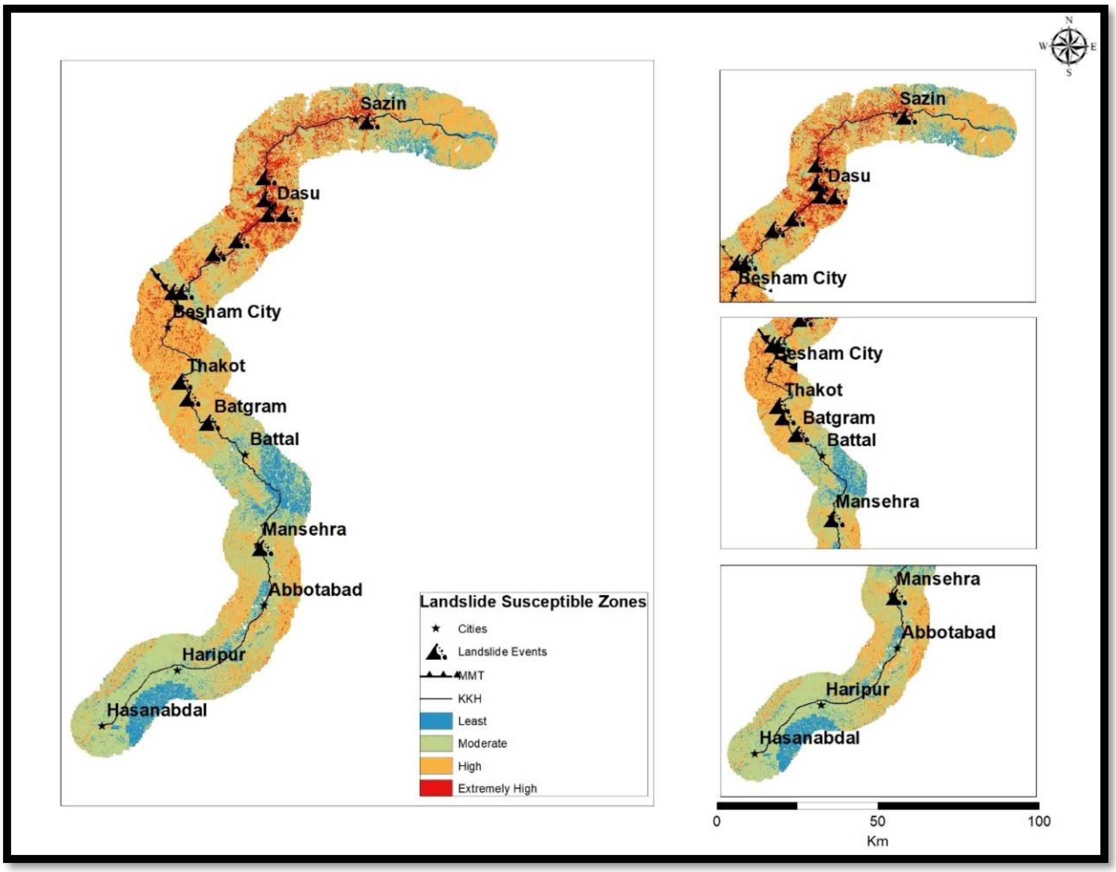

Figure 8. Landslide susceptibility map depicting susceptible zones.

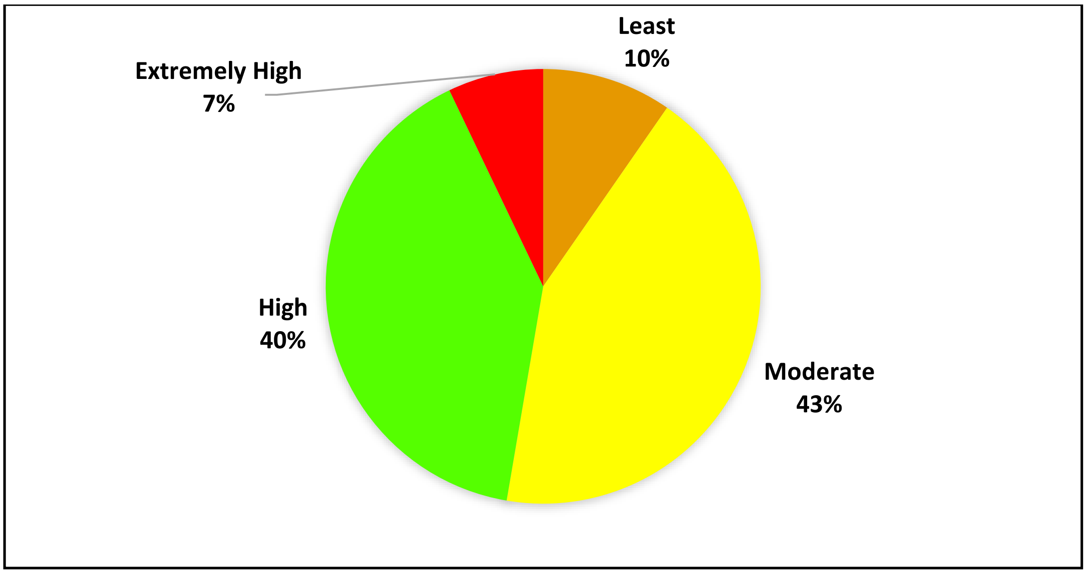

Figure 9. Piechart of the landslide susceptibility zones of study area.

Table 7. Validation of the Landslide Susceptibility Map by using known landslide areas.

Group	**Landslide Events**	**Pixels**	**Low**	**Moderate**	**High**	**Extremely High**
1	**LS1**	7	0	0	0	7
2	**LS2**	9	1	7	1	0
3	**LS3**	11	0	3	4	4
4	**LS4**	5	0	2	3	0
5	**LS5**	4	0	0	0	4
6	**LS6**	10	0	0	4	6
7	**LS7**	8	0	0	4	4
8	**LS8**	5	0	0	0	5
9	**LS9**	3	0	0	2	1
10	**LS10**	2	0	0	1	1
11	**L11**	3	0	2	0	1
12	**LS12**	2	0	1	0	1
	Area (%)	69	1.5	21.7	27.5	49.2

The least stable surfaces were included the majority of the region with a steep slope. According to the broad range volume search, the unstable sites show little resemblance to the slope map. A separate volume was associated with each critical surface. In the moderate volume search, the majority of the critical surfaces lie around the higher limits whereas, the higher volume search showed that the area is mostly covered with the critical surfaces in the areas that are seismologically active sites. Some of the studies (Mahmood 2016; Ali S et al. 2017) that have undertaken probabilistic approaches of limit equilibrium for the slope stability in Northern Pakistan are different from the findings of this research. This is because slope stability through Scoops 3D incorporates a series of triggering factors along with the effects of slope and it also caters the 3D geometry and geological structures of the region. After interpolation of the derived values from Scoops 3D model, the results predicted that almost 3952 km of the study area is likely to be affected by the landslides.

The validation of the findings from the current study showed that the findings are slightly different from that obtained from AHP. The susceptible zones identified through Scoops 3D does not only represent the landslide-prone sites but also the level of mass failures. Table 4 summarized the validation of the findings from Scoops 3D. The presence of Main Mantle Thrust along the Kohistan region tends to show that the cities around this seismologically active zone can result in landslides so intense that include boulder falls (Ali S et al. 2017). Around the southern region of KKH, Abbottabad, and Hasanabdal areas are mostly hit by landslides comprising of debris flow and since the area also receives maximum rainfall, so the landslides are precipitation induced (Mahmood 2016). Hence, Scoops 3D can be utilized as a suitable methodology for slope stability because of its feasibility of incorporating steep slopes, weak materials, and pore pressure values.

Interpretation of the Results with the association to KKH

For interpretation purpose, the study area has been divided into three sections, i.e. Hasanabdal-Manshera, Manshera-Besham city, and Besham-Sazin onward. The Hasanabdal-Manshera region along the KKH distinguished by Quaternary age material (alluvial, glaciofluvial deposits, morainic, & debris-flow) with very gentle-gentle to moderate slope, with annual mean precipitation range of 246 mm to 1328 mm (highest in Abbottabad region 1074 mm to 1328 mm & lowest in the Hasanabdal region), dominated by urban, forest, vegetation land use/land cover classes. This region has been classified as low to moderate landslide susceptibility zones. The most common types of landslides in this region is comprised of the rotational slide, transitional slide, mudflow, earthflow, debris flow and occasionally rockfall. The main reason for these types of landslides could be because this region receives the highest amount of rainfall during the summer monsoon period (July-September) and westerly disturbances during the winter season. The soils of this region are mainly comprised of clayey and loamy soils mainly non-calcareous belong to the soil order Inceptisols & Alfisols (chromudertic subgroup), these soils may have montmorillonitic types of clay minerals which have the highest wetting & swelling hydraulic properties. Heavy rainfall leads to saturation of slopes is a major cause of the landslide.

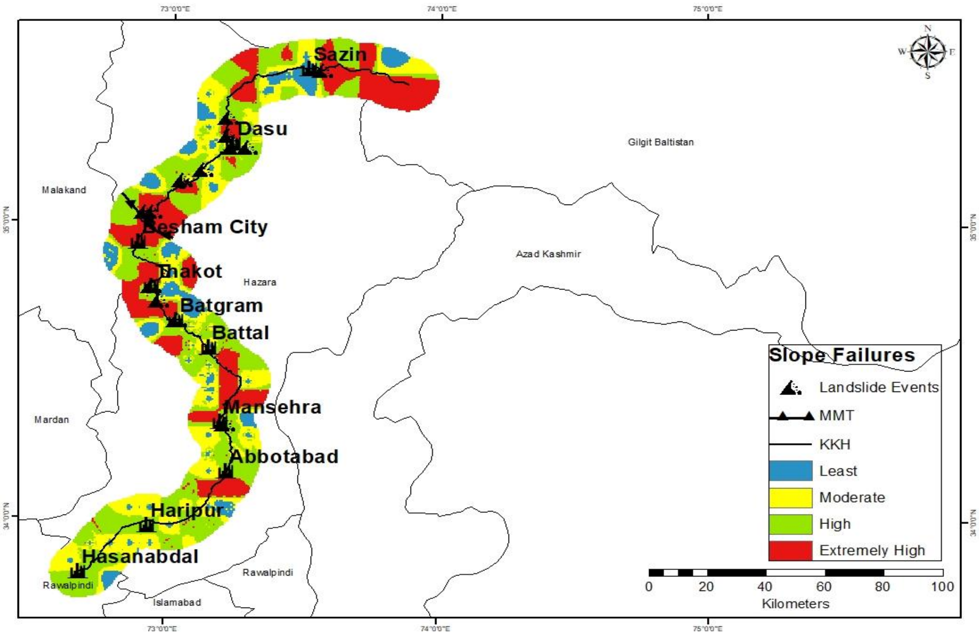

Figure 10. The volume of potential slope failures along the study area

Table 8. Validation of Scoops 3D results using the inventory data.

Landslide Events	Area (Km)	Percentage
LS1	336	8.5
LS2	319	8.07
LS3	336	8.5
LS4	312	7.9
LS5	308	7.8
LS6	310	7.8
LS7	343	8.6
LS8	320	8.09
LS9	328	8.2
LS10	337	8.5
LS11	335	8.4
LS12	368	9.3
Total	3952	100

This is further aggravated for example in the Abbottabad region after the October 8, 2008, mega earthquake which led to significant changes in land use/land cover. About a 10% increase in settlement in Abbottabad region was observed due to resettlement from earthquake-affected areas this had not only affected the forested area but also increased farming on the steeper slopes.

The Mansehra-Besham city section of KKH is characterized as Precambrian (Quartz-mica schist, phyllitic slates with subordinate white marble bands) & Cambrian (Granitic gneiss) age material with gentle to moderately steep to steep slope, with annual mean precipitation range of 246 mm to 1074 mm (highest in Besham city region 1074 mm & 246 mm lowest in the Battle region), dominated by urban, vegetation land use/land cover classes. This region has been classified as moderate to high landslide susceptibility zones. The most common types of landslides in this region is comprised of rockfall, topple and debris flow, and earthflow. The main triggering factors of these types of landslides in this area are monsoonal summer heavy rainfall and their proximity to MMT line transecting the KKH at Besham city area.

The Besham-Sazin region of KKH is characterized by diverse geological periods comprising of Cretaceous to Jurassic, Cambrian and Precambrian rocks. These rocks predominantly include the Schists, Quartzite, Marble, Granite and Mafic-Ultra Mafic cumulates. This region receives least to high annual precipitation (least in Chilas region 246mm and high in Besham region 1074 mm) and is covered with valleys and natural forests. This region has been categorized in the Moderate to extremely high susceptible landslide zones. The standard type of landslides in this region is mudflow and boulders and rockfall. However, towards the north of the study area, the regions of Shatial and

Summer are susceptible to the risk of avalanches. The significant triggering landslide factors are the geology of this region that includes the proximity to MMT and the type of lithology.

The results are in line with the study that supports steep slope the landslide susceptibility increases(Shrestha et al. 2004). Following the geology, the other triggering factor for landslides in this area is the precipitation. Yalcin in his study has explained such meteorological parameters like the extent of sunshine, rainfall direction, the morphology of the surface, aspect areas and directly facing the river and roads make the area even more susceptible to landslides (Yalcin 2008). The anthropogenic cause is another critical parameter that can cause the landslides by the constant and intensive change in the land cover. The factors of curvature, aspect, and elevation are also incorporated in the assessment of landslide susceptibility as their significance is mentioned in the literature (Rashid A 2004; Ahmed et al. 2014; Kanwal et al. 2017).

Since the current study mainly focused on the areas around the highway and how the landslides affect the region, several studies show the degree of landslide susceptibility increases as the proximity to roads decreases (Moradi et al. 2012; Bagherzadeh and Daneshvar 2013). Moreover, the presence of healthy roots and thick forests make the area less susceptible to landslide because it provides better anchorage against the soil erosion (Komac 2006; Leventhal and Kotze 2008; Bathrellos et al. 2009; Neuhäuser et al. 2012). This can be observed in this study that the region covered with dense forests in the Southern region is less susceptible to landslides whereas the northern region of the study area is highly susceptible to landslides.

Susceptibility map validation techniques are usually implied to compare susceptibility map with the already occurred landslide incidents and accepted that future landslide will occur in the same sites as the existing places (Kamp et al. 2008; Khattak et al. 2010). Lastly, a landslide susceptibility map generated using AHP technique was validated with the Google Earth imagery and geological survey of Pakistan landslides inventory map. The zonal pie chart is shown in the Fig. 6 represents the landslides area by superimposing and visually inspecting the maps. Table 3 shows the results of validation and it's concluded that around 49.2% of the known landslides have occurred in the predicted area that comes under the extremely high susceptibility zone whereas 27.5 %, 21.5 %, and 1.5% falls in the high, moderate and low susceptible regions respectively.

Comparison of AHP and Scoops 3D

Basically, both Analytical Hierarchy Process and Scoops Model are capable of monitoring the landslide susceptibility sites. AHP is a multi-criterion decision based process model whereas the Scoops is a process model that takes into account different subsurface parameters and after various simulations can yield a precise results regarding the slope failures. However, an in-depth methodical approach is provided by Scoops to assess the slope stability which provides a detailed account of the volume or the area of the potential landslides. A possible limitation of Scoops in the limit equilibrium analysis, it only offers two methods, Fellinious and Bishop’s method and only rotational slides are considered while calculating the slope failures. Both these models can collectively be used for calculating the susceptible zones as identifying the potential failure size and area. The Table 9 summarizes the capabilities of AHP and Scoops.

Table 9. Comparison of the abilities of AHP and Scoops for landslide susceptibility of the study area.

	Scoops 3D	**AHP**
Model Type	Process Model that utilizes DEM and limit equilibrium technique to assess the slope stability.	Multi criteria decision model that utilizes ranks and weights.
3d Approach	Applies the 3d approach by incorporating shear strength, internal friction, and pore pressure.	Doesn't incorporate any subsurface properties of strength, internal friction or pore pressure.
User-defined criteria	Yes, the size of potential failure is according to the user's input. The potential failures are either represented in area or volume.	No, it only gives the susceptible zones without any information about potential failure sizes.
Groundwater Conditions	A variety of options for incorporating groundwater conditions in slope stability analysis is used in this model.	Diverse groundwater properties cannot be included in technique.
Seismic Loading	Seismic loading effects can be incorporated in the pseudo-static analysis.	The presence of thrust and fault lines can only be incorporated into the analysis.
Computational Efficiency	Computational efficiency is enhanced by coarse to fine search technique.	Enhancement of computational efficiency is not possible in this case until the influencing factors are decreased.

Chapter 4

CONCLUSION AND RECOMMENDATIONS

4.1 Conclusions

The research provides deforestation and forest degradation statistics along 10-km of Karakoram Highway originating from Hasanabdal to Sazin region over a period of 25 years. The study employed a consistent dataset and methodology. The results displayed a noteworthy increase in deforestation trend. The forest cover has shown a 26 % decrease from 1990 to 2016. However, the reserved forests along the area remain undisturbed. The results showed that geospatial techniques are useful in monitoring and counteracting the spatiotemporal changes in the land use land cover. The accuracy assessment results were reassuring and hopeful for the adopted approach of supervised classification. The deforestation in the area can be attributed to violation of environmental laws, poor forest management and non-conductance of proper Environmental Impact Assessment. The forest degradation hotspots recognized in this study encourages further research to study the underlying deforestation drivers. The quantitative research on underlying factors causing the degradation using spatiotemporal analysis can promote effective and inclusive forest management strategies. Furthermore, this subject would garner more consideration in future research (Rashid B and Iqbal 2018).

In the current study, a combined approach of quantitative index based on the Analytical Hierarchical Process and Weighted Linear Combination was used to map the landslide susceptibility of the Karakoram Highway. The empirical evaluation represented that slope and lithology are the key factors to determine landslides followed by precipitation and anthropogenic interventions in the form of clearings done for urban settlements. The assessed area was broadly categorized into four susceptibility zones low, moderate, high and extremely high that showed almost 43% in moderate and 40% in high susceptible zone whereas only 7% in extremely high and 10 % in the low susceptibility zone. The quality of the final output relies significantly on the input causative layers, but the process is convenient and easy to update and get the rapid results. Scoops provided a quantified approach to assess the contribution of the slope and lithology of the area in estimating the volume of the slope failures. The earthquake loading information under dry conditions was incorporated in the analysis and three categories of slope failures in the volume defined as low, moderate and high mass. The results produced by the AHP and Scoops 3D susceptibility map coincide with the known landslide occurrence site. Hence, the results can be utilized as a base map for landslide assessment and evaluation to aid in decision making and developmental activities. Both the AHP based landslides and Scoops 3D based landslides assessment can be utilized for the explanation of causative factors for triggering and causing landslides, thus, corroborating in mitigation of future landslide hazards along the Karakoram Highway.

4.2 Recommendations for further research

The methodology described in the current research can be utilized to monitor the deforestation hotspots and landslide susceptible zones of individual cities that fall along the study area. Afforestation and Reforestation drive should be encouraged particularly in the study area and generally in the country. The concerned authorities need to identify the forest resources rights clearly, formulate community management systems and legal framework that monitors, records and reports each act and violations transparently (Rashid & Iqbal 2018). The concerned forest management authorities and the hazards and risk management departments need to ensure efficient and optimal effort to counter the damage and prevent any more loss of the biodiversity of the area. Deforestation and landslides should be measured annually. Geotechnical surveys should be done in order to help in preventive measures in the affected areas. The construction of buildings and extensive removal of forests needs to be discouraged in the vulnerable zones. Proper guidelines and precautions should be followed if there is a need for a land cover shift. The current study is subject to the causative parameters of LULC, rainfall, lithology and DEM derivatives; it could be verified and modified in the future by the addition of hydrologic and soil properties factors. Scoops is a new approach in the slope stability analysis. Along with accurate geotechnical data, it can yield better results. So further research should be encouraged in this direction. Other landslide susceptibility mapping approaches like statistical modeling can be adapted to identify the risk-prone areas.

REFERENCES

1) A.W., B. (1955). *The use of slip circle in the stability analysis of slopes* (1 ed. Vol. 5).
2) Ahmed, M. F., Rogers, J. D., & Ismail, E. H. (2014). A regional level preliminary landslide susceptibility study of the upper Indus river basin. *European Journal of Remote Sensing, 47*(1), 343-373. doi:10.5721/EuJRS20144721
3) Ali, S., Schneiderwind, S., & Reicherter, K. (2017). *Structural and Climatic Control of Mass Movements Along the Karakoram Highway.* Paper presented at the Workshop on World Landslide Forum.
4) Ali, T., Shahbaz, B., & Suleri, A. (2006). Analysis of myths and realities of deforestation in Northwest Pakistan: implications for forestry extension. *International Journal of Agriculture and Biology, 8*(1), 107-110.
5) Ayalew, L., & Yamagishi, H. (2005). The application of GIS-based logistic regression for landslide susceptibility mapping in the Kakuda-Yahiko Mountains, Central Japan. *Geomorphology, 65*(1-2), 15-31.
6) Ayalew, L., Yamagishi, H., & Ugawa, N. (2004). Landslide susceptibility mapping using GIS-based weighted linear combination, the case in Tsugawa area of Agano River, Niigata Prefecture, Japan. *Landslides, 1*(1), 73-81. doi:10.1007/s10346-003-0006-9
7) Bagherzadeh, A., & Daneshvar, M. R. M. (2013). Mapping of landslide hazard zonation using GIS at Golestan watershed, northeast of Iran. *Arabian Journal of Geosciences, 6*(9), 3377-3388.
8) Basa, N., Shafique, M., Bacha, A. S., Shah, S. U., Basharat, M., Ali, M. Z., . . . Khan, S. (2016). Landslides induced vulnerability and risk assessment in Muzaffarabad and Balakot, Pakistan. *Journal of Himalayan Earth Science, 49*(2).
9) Bathrellos, G. D., Kalivas, D., & Skilodimou, H. D. (2009). GIS-based landslide susceptibility mapping models applied to natural and urban planning in Trikala, Central Greece. *Estud Geol, 65*(1), 49-65.
10) Brabb, E. (1993). *Proposal for worldwide landslide hazard maps.* Paper presented at the Proceedings 7th international conference and field workshop on landslides. S. Novosad and P. Wagner (eds.), Balkema, Rotterdam.
11) Cannon, S. (1993). *Empirical model for the volume-change behavior of debris flows.* Paper presented at the Proceedings of the National Conference on Hydraulic Engineering.
12) Cardinali, M., Reichenbach, P., Guzzetti, F., Ardizzone, F., Antonini, G., Galli, M., . . . Salvati, P. (2002). A geomorphological approach to the estimation of landslide hazards and risks in Umbria, Central Italy. *Natural hazards and earth system science, 2*(1/2), 57-72.
13) Champatiray, P. (2000). Perationalization of cost-effective methodology for landslide hazard zonation using RS and GIS: IIRS initiative. *Natural Disasters and their mitigation*, 95-101.

14) Chang, K.-T., & Chiang, S.-H. (2009). An integrated model for predicting rainfall-induced landslides. *Geomorphology, 105*(3-4), 366-373.
15) Colombo, A., Lanteri, L., Ramasco, M., & Troisi, C. (2005). Systematic GIS-based landslide inventory as the first step for effective landslide-hazard management. *Landslides, 2*(4), 291-301.
16) Daneshvar, M. R. M. (2014). Landslide susceptibility zonation using analytical hierarchy process and GIS for the Bojnurd region, northeast of Iran. *Landslides, 11*(6), 1079-1091.
17) Duncan, J., & Wright, S. (1980). The accuracy of equilibrium methods of slope stability analysis. *Engineering geology, 16*(1-2), 5-17.
18) Ercanoglu, M. (2005). Landslide susceptibility assessment of SE Bartin (West Black Sea region, Turkey) by artificial neural networks. *Natural Hazards and Earth System Sciences, 5*(6), 979-992.
19) Fannin, R., & Wise, M. (2001). An empirical-statistical model for debris flow travel distance. *Canadian Geotechnical Journal, 38*(5), 982-994.
20) FAO. (2006). Global Forest Resources Assessment 2005. *FAO Forestry Paper, 147*.
21) FAO. (2010). Global forest resources assessment. *Main report, FAO Forest paper 163*.
22) FAO. (2015). *Global Forest Resources Assessment 2015: How are the World's Forests Changing?* : Food and Agriculture Organization of the United Nations.
23) Feizizadeh, B., Blaschke, T., Nazmfar, H., & Rezaei Moghaddam, M. (2013). Landslide susceptibility mapping for the Urmia Lake basin, Iran: a multi-criteria evaluation approach using GIS. *International Journal of Environmental Research, 7*(2), 319-336.
24) Fell, R., Corominas, J., Bonnard, C., Cascini, L., Leroi, E., & Savage, W. Z. (2008). Guidelines for landslide susceptibility, hazard and risk zoning for land use planning. *Engineering geology, 102*(3), 85-98.
25) Fischer, K. M., Khan, M. H., Gandapur, A. K., Rao, A. L., M., Z. R., & Marwat, H. (2010). *Study on timber harvesting ban in NWFP, Pakistan*: Intercooperation Pakistan.
26) Gilani, H., Murthy, M., Bajracharya, B., Karky, B., Koju, U., Joshi, G., . . . Sohail, M. (2015). Assessment of change in forest cover and biomass using geospatial techniques to support REDD+ activities in Nepal. *ICIMOD Working Paper*(2015/5).
27) Gorsevski, P. V., Gessler, P. E., Boll, J., Elliot, W. J., & Foltz, R. B. (2006). Spatially and temporally distributed modeling of landslide susceptibility. *Geomorphology, 80*(3-4), 178-198.
28) Guzzetti, F., Carrara, A., Cardinali, M., & Reichenbach, P. (1999). Landslide hazard evaluation: a review of current techniques and their application in a multi-scale study, Central Italy. *Geomorphology, 31*(1), 181-216.
29) Haeusler, T., Schnurr, J., & Fischer, K. (2000). Provincial Forest Resource Inventory (PFRI) North West Frontier Province—Pakistan. *Google Scholar*.
30) Haigh, M. (1984). Landslide prediction and highway maintenance in the Lesser Himalaya, India. *Zeitschrift f. ur Geomorphology NF, 51*, 17-37.

31) Hamilton, L. (2008). Forests and water: a thematic study prepared in the framework of the Global Forest Resources Assessment 2005. Rome: Food and Agricultural Organization, United Nations; 2008. In.
32) Hung, L. Q., Van, N. T. H., Van Son, P., Khanh, N. H., & Binh, L. T. (2016). Landslide susceptibility mapping by combining the analytical hierarchy process and weighted linear combination methods: a case study in the upper Lo River catchment (Vietnam). *Landslides*, *13*(5), 1285-1301.
33) Hungr, O., Salgado, F., & Byrne, P. (1989). Evaluation of a three-dimensional method of slope stability analysis. *Canadian Geotechnical Journal, 26*(4), 679-686.
34) Intarawichian, N., & Dasananda, S. (2010). Analytical hierarchy process for landslide susceptibility mapping in lower Mae Chaem Watershed, Northern Thailand. *Suranaree Journal of Science & Technology, 17*(3).
35) IPCC. (2013). Climate change 2013: the physical science basis. Intergovernmental panel on climate change, working group I contribution to the IPCC fifth assessment report (AR5). *New York*.
36) Jibson, R. W., & Jibson, M. W. (2003). *Java programs for using Newmark's method and simplified decoupled analysis to model slope performance during earthquakes*: Geological Survey (US).
37) Kamp, U., Growley, B. J., Khattak, G. A., & Owen, L. A. (2008). GIS-based landslide susceptibility mapping for the 2005 Kashmir earthquake region. *Geomorphology, 101*(4), 631-642.
38) Kanungo, D., Arora, M., Sarkar, S., & Gupta, R. (2012). Landslide Susceptibility Zonation (LSZ) Mapping–A Review.
39) Kanwal, S., Atif, S., & Shafiq, M. (2017). GIS based landslide susceptibility mapping of northern areas of Pakistan, a case study of Shigar and Shyok Basins. *Geomatics, Natural Hazards and Risk, 8*(2), 348-366.
40) Khattak, G. A., Owen, L. A., Kamp, U., & Harp, E. L. (2010). Evolution of earthquake-triggered landslides in the Kashmir Himalaya, northern Pakistan. *Geomorphology*, *115*(1-2), 102-108.
41) Komac, M. (2006). A landslide susceptibility model using the analytical hierarchy process method and multivariate statistics in perialpine Slovenia. *Geomorphology, 74*(1-4), 17-28.
42) Ladas, I., Fountoulis, I., & Mariolakos, I. (2007). Using GIS and multicriteria decision analysis in landslide susceptibility mapping-a case study in Messinia prefecture area (SW Peloponnesus, Greece). *Bulletin of the Hellenic Geological Society, 40*(4), 1973-1985.
43) Lam, L., & Fredlund, D. (1993). A general limit equilibrium model for three-dimensional slope stability analysis. *Canadian Geotechnical Journal, 30*(6), 905-919.
44) Lei, G. H., Chiu, A. C. F., and , & Zheng, Q. (2011). *Understanding the limitations of the Swedish method of slices from the stress perspective*. Paper presented at the Proceedings of the 14th Pan-American Conference on Soil Mechanics and Geotechnical Engineering, Toronto.

45) Leventhal, A. R., & Kotze, G. P. (2008). Landslide susceptibility and hazard mapping in Australia for land-use planning—with reference to challenges in metropolitan suburbia. *Engineering geology, 102*(3-4), 238-250.
46) Lund, H. G. (2002). When is a forest not a forest? *Journal of Forestry, 100*(8), 21-28.
47) Mahmood, K. (2016). Probabilistic Slope Stability Analysis of Landslide at Abbottabad Pakistan.
48) Mashhadifarahani, S. (2015). Applying GIS and Remote Sensing Techniques to Predict Landslides. *Indian Journal of Science and Technology, 8*.
49) Mondal, S., & Maiti, R. (2012). Landslide susceptibility analysis of Shiv-Khola watershed, Darjiling: a remote sensing & GIS based Analytical Hierarchy Process (AHP). *Journal of the Indian Society of Remote Sensing, 40*(3), 483-496.
50) Moradi, M., Bazyar, M. H., & Mohammadi, Z. (2012). GIS-based landslide susceptibility mapping by AHP method, a case study, Dena City, Iran. *Journal of Basic and Applied Scientific Research, 2*(7), 6715-6723.
51) Nagarajan, R., Roy, A., Kumar, R. V., Mukherjee, A., & Khire, M. (2000). Landslide hazard susceptibility mapping based on terrain and climatic factors for tropical monsoon regions. *Bulletin of Engineering Geology and the Environment*, *58*(4), 275-287.
52) Neuhäuser, B., Damm, B., & Terhorst, B. (2012). GIS-based assessment of landslide susceptibility on the base of the weights-of-evidence model. *Landslides*, *9*(4), 511-528.
53) Newmark, N. M. (1965). Effects of earthquakes on dams and embankments. *Geotechnique, 15*(2), 139-160.
54) Nilsen, T. H. (1979). *Relative slope stability and land-use planning in the San Francisco Bay region, California* (Vol. 944): US Govt. Print. Off.
55) Pan, X., Nakamura, H., Nozaki, T., & Huang, X. (2008). A GIS-based landslide hazard assessment by multivariate analysis. *Journal of the Japan landslide society*, *45*(3), 187-195.
56) Pradhan, B., & Lee, S. (2010). Regional landslide susceptibility analysis using back-propagation neural network model at Cameron Highland, Malaysia. *Landslides, 7*(1), 13-30.
57) Preuth, T., Glade, T., & Demoulin, A. (2010). Stability analysis of a human-influenced landslide in eastern Belgium. *Geomorphology*, *120*(1-2), 38-47.
58) Qamer, F. M., Shehzad, K., Abbas, S., Murthy, M., Xi, C., Gilani, H., & Bajracharya, B. (2016). Mapping deforestation and forest degradation patterns in western Himalaya, Pakistan. *Remote Sensing, 8*(5), 385.
59) Rashid, A. (2004). Impact of El-Nino on summer monsoon rainfall of Pakistan. *Pakistan Journal of Meteorology, 1*(2).
60) Rashid, B., & Iqbal, J. (2018). Spatiotemporal change detection in forest cover dynamics along landslide susceptible region of Karakoram Highway, Pakistan *ISPRS Annals of Photogrammetry, Remote Sensing & Spatial Information Sciences, 4*(3).

61) Raza, A., Raja, I. A., Raza, S., & Lindgren, E. (2012). Land-use change analysis of district Abbotabad Pakistan: Taking advantage of GIS And remote sensing. *A scientific journal of COMSATS – Science Vision, 18*.
62) Reid, M. E., Christian, S. B., & Brien, D. L. (2000). Gravitational stability of three-dimensional stratovolcano edifices. *Journal of Geophysical Research: Solid Earth, 105*(B3), 6043-6056.
63) Reid, M. E., Christian, S. B., Brien, D. L., & Henderson, S. (2015). Scoops3D—Software to Analyze Three-Dimensional Slope Stability Throughout a Digital Landscape. In *Tech. Rep. US Geological Survey Techniques and Methods, book 14* (pp. 218).
64) Saaty, T. L. (1980). The analytic hierarchy process: planning, priority setting, resources allocation. *New York: McGraw, 281*.
65) Saaty, T. L., & Vargas, L. G. (2000). Models, Methods, Concepts & Applications of the Analytic Hierarchy Process, International Series in Operations Research and Management Science, 34. In: Kluwer, Boston.
66) Saboya Jr, F., da Glória Alves, M., & Pinto, W. D. (2006). Assessment of failure susceptibility of soil slopes using fuzzy logic. *Engineering geology, 86*(4), 211-224.
67) Şener, Ş., Sener, E., & Karagüzel, R. (2011). Solid waste disposal site selection with GIS and AHP methodology: a case study in Senirkent–Uluborlu (Isparta) Basin, Turkey. *Environmental monitoring and assessment, 173*(1-4), 533-554.
68) Shrestha, D., Zinck, J., & Van Ranst, E. (2004). Modelling land degradation in the Nepalese Himalaya. *Catena, 57*(2), 135-156.
69) Siddiqui, K. (1997). Asia-pacific forestry sector outlook study. *Forestry Policy and Planning Division, Rome, regional Office for Asia and the Pacific, Bangkok*.
70) Sorbino, G., Sica, C., & Cascini, L. (2010). Susceptibility analysis of shallow landslides source areas using physically based models. *Natural hazards, 53*(2), 313-332.
71) Tejwani, K. (1987). Sedimentation of reservoirs in the Himalayan region: India. *Mountain Research and Development*, 323-327.
72) Travasarou, T., Bray, J. D., & Abrahamson, N. A. (2003). Empirical attenuation relationship for Arias intensity. *Earthquake engineering & structural dynamics, 32*(7), 1133-1155.
73) Varnes, D. J. (1984). *Landslide hazard zonation: a review of principles and practice*.
74) Wagner, A., Leite, E., & Olivier, R. (1988). *Rock and debris-slides risk mapping in Nepal–A user-friendly PC system for risk mapping.* Paper presented at the Proceedings of the 5th International Symposium on Landslides.
75) Waseem, M., Javed, W., Ahmad, I., Khan, M. A., & Ur-Rehman, F. (2013). Deterministic seismic hazard analysis of Peshawar. *Journal of Himalayan Earth Sciences, 46*(1).
76) Xu, C., Dai, F., Xu, X., & Lee, Y. H. (2012). GIS-based support vector machine modeling of earthquake-triggered landslide susceptibility in the Jianjiang River watershed, China. *Geomorphology, 145*, 70-80.

77) Yalcin, A. (2008). GIS-based landslide susceptibility mapping using analytical hierarchy process and bivariate statistics in Ardesen (Turkey): comparisons of results and confirmations. *Catena*, *72*(1), 1-12.
78) Yann le Polain, D. W., & Lambin, E. F. (2012). Monitoring degradation in arid and semi-arid forests and woodlands: the case of the argan woodlands (Morocco). *Applied Geography*, *32*(2), 777-786.

APPENDICES

Appendix 1 Lithology of the study area

Types of Crust	Symbols of Mineral	Descriptions
Quatenary	Qal Qgf	Alluvium Glaciofluvial deposits
Cretaceous	Kkkp Kkkgd Kkd Kkhgd Kktz Ksc Kcs Kcq Krv Krm Kts Ktm Kgf Kcd Kcsgb Kcgb Kcm Kcu	Granodiorite with pegmatite and aplite Granodiorite and diorite Diorite and granodiorite Granodiorite, granite with few aplite and pegmatite dykes Ophiolitic mélange (Ultramafic, metabasalts, metesediment and turbidites) Conglomerates have arenaceous and calcareous pebbles and cobbles Schist, slate, phyllite and marble bands Quartzite Volcanics, mostly andesite, basalt and tuff metamorphosed into amphibolite with minor metasediments Slate, Schist, marble and metavolcanices Slates, Phyllitic schists, green schists and quartzite Marble Schists, paragneisses with minor amphiboilite, calc-silicates, granites, pegmatite and aplite Diorite Sheared gabbronorite (amphibolite and green schist Gabbronorite, gabbro and diorite Troctolite (layered) and gabbronorite Mafic-ultramafic cumulate (dunite, wehrlite, gabbro, gabbronorite and anorthosite)
Cretaceous to Jurassic	Jgd	Dolomite and dolomitic limestone with minor slate
Permian	Pms Pmph Pm Pmq Pkl Pks Pga	Mostly slate with minor quartzite and limestone Phyllite with minor slate, quartzite and limestone Limestone with minor slate and quartzite Quartzite with minor slate and limestone Limestone and dolomitic limestone with minor slates Slates Argillite interbedded with dolomitic limestone and quartzite
Carboniferous	Cps	Slate with minor quartzite and limestone
Precambrian	PEbgn	Orthogneiss and migmatites with pegmatite and aplite

	PEbm	Lime-silicate marble with paragneiss, pegmatite and aplite
	PEbsc	Phyllitic schist, schist and gneisses (ranging from biotite to silliminite grade) and marble
	PEb	Schists, Impure quartzite, gneisses mostly cataclastic type; intruded by younger granite and pegmatite and amphibiotized dykes
	PEt	Quartz-mica schist, Phyllitic slates with subordinate white marble bands
	PEh	Black to khaki slates, brown phyllite, greywackes, siltstone
	PEngn	Granitic gneisses (augen and banded gneisses) with minor metasediments.
Tertiary	Tkgr	Diorite, granite, pegmatite and aplite
	Kkt	Tonallite
	Kko	Orthogneiss
	TlI	Light to dark grey, nodular limestone (Paleocene)
Jurassic	Jka	Garnet-bearing amphibolite (massive and sheared)
	Jkba	Garnet-free amphibolite(banded)
	Jjggb	Garnet gabbro
	Jjpy	Garnet pyroxenite
	Jjd	Dunite
	Jjpy	Pyroxenite and serpentinite
Cambrian	Emgr	Porphyitic granite
	Emgrgn	Granitic gneiss
	Eaf	Basal conglomerate, limestone, dolomite with cherty bands at places dolomitic limestone, sandstone, shale

Appendix 2 Areas Along KKH


BONARDAS